UCRL 15600
S/C 7247001

# WIDE SPECTRUM ANTIREFLECTIVE COATING FOR LASER FUSION SYSTEMS -- FINAL REPORT

UCRL--15600

DE84 013211

B. E. Yoldas, D. P. Partlow, H. D. Smith*,
D. M. Mattox
Westinghouse R&D Center

*Westinghouse Hanford Company

January 13, 1984

## DISCLAIMER



Westinghouse R&D Center
1310 Beulah Road
Pittsburgh, Pennsylvania 15235

## 1. INTRODUCTION AND BACKGROUND INFORMATION

The goal of the Laser Fusion Program at the Lawrence Livermore National Laboratory (LLNL) is to produce a well-diagnosed thermonuclear implosion using a Nd glass solid state laser. For this purpose, the NOVA laser was originally designed to provide 200 to 300 kJ on target at 1.05 μm (1ω). Experiments with the Argus, Shiva and Novette laser systems have demonstrated the advantages of short wavelength laser driven systems. Operation at the first (1ω) and second (2ω) harmonics of the Nd laser, 1.05 μm and 0.53 μm, respectively, presents no outstanding problem for the optical system, since glasses with excellent transmission at these wavelengths are available, and methods of forming antireflective (AR) surfaces on these glasses are well known. Operation at the third harmonic, 0.35 μm (3ω), however, requires lenses and windows of fused silica, since other available glasses absorb light at these short wavelengths. Advanced surface treatment methods for forming AR surfaces, such as leaching of phase separated glasses, and Schott's Neutral Solution Process cannot be applied to fused silica, because it is a single phase glass. But operation of the laser system without an AR coating on the fused silica lenses causes substantial energy loss, since there are numerous lenses and windows in series. For this reason, The University of California subcontracted a project to Westinghouse to develop an AR coating on fused silica lenses with an additional requirement that the AR coating be laser damage resistant at 0.35 μm.

Reflection of radiation at the interface between two transparent media can be calculated from Fresnel's equation. For normal incidence in an air environment, Fresnel's equation simplifies to

*University of California Subcontract No. 7247001, under technical direction of the Lawrence Livermore National Laboratory.

$R = (n - 1 / n + 1)^2$ where R is the reflectance and n is the index of refraction of the substrate. For example, fused silica has an index of refraction of 1.477 at 0.35 μm; thus its reflectance at this wavelength is approximately 7.5%. If the radiation at this wavelength passes through, for example, six optical components, then over one-third of the initial energy is lost due to surface reflection. When delivery of maximum energy to the target is a key element in the success of the work, which is the case in laser-induced fusion experiments, this loss of energy becomes economically intolerable, and an antireflective coating is needed.

Lord Rayleigh[1] and Fraunhofer[2] observed almost a century ago that the surface reflection of glass can be reduced by chemical treatment of the surface. Later, a method of forming antireflective films by acid treatment of the glass surface was introduced.[3-7] However, many of these films were reported either to be unstable or not to show an increase in transmission corresponding to the decrease in reflection. A transparent material whose index of refraction is equal to the square root of that of the glass, when deposited as a quarter wavelength thick film on that glass, provides an interference minimum in the reflectivity at the chosen wavelength. This idea was first expressed by G. Bauer,[8] and similar antireflective films were formed on glass by various workers.[9-13] A typical glass has an index of refraction between ∿1.45 and 1.65, which implies that the index of refraction of the antireflective interference film must be between 1.20 to 1.25. This low-index requirement makes it practically impossible to design a dense single layer AR film on glass.

Fortunately, the problem can be treated in another way. Since the index of refraction of a material is related to its density, the index can be lowered by introducing porosity. It is required, however, that the pore size be substantially smaller than the wavelength of the light, and that the pore distribution be homogeneous in order not to affect the light transmission and cause scattering.

The porosity and index of refraction in this type of material are related by[14]

$$n_p^2 = (n^2-1)(1-P) + 1 \qquad (1)$$

where $n_p$ and $n$ are indices of the porous and non-porous materials and P is the volume fraction of non-scattering porosity.

If a homogeneous single-layer film, antireflective at the 350 nm wavelength, were to be formed on fused silica, this layer would have to have an index of refraction of 1.215 (the square root of the substrate index), and a thickness of 72 nm ($t_c = \lambda/4\, n_c$). To attain this low index in a $SiO_2$ film, a non-scattering porosity of ~60% must be introduced (from Eq. 1). It is doubtful that such a large porosity can be introduced into a 75 nm thick film. Homogeneous single-layer AR films also require precise thickness control. However, if the porosity (and therefore the index) were to be graded, wide spectrum antireflectivity could be attained with a much lower total porosity, and the performance of such films would become much less sensitive to thickness variations.

Introduction of porosity in a glass surface layer may be accomplished in various ways. Such porous layers have been formed by chemical leaching of a phase separated glass or by neutral solution processing, both of which are applicable only to specific glass compositions.[15-18] Some of the drawbacks to using these types of glass with short-wavelength, high-power lasers are discussed by Lowdermilk, et al.[19] Deposition of optical oxide films from metal-organic compounds is also known.[20-22] This method has the advantage that the coating is essentially independent of substrate composition. The requirement that the coating be non-absorbing at 350 nm for the NOVA laser system limits the coating material to a few oxides, e.g., $SiO_2$, $Al_2O_3$, $La_2O_3$, $ThO_2$, HfO . All of these oxides except $SiO_2$ have a rather high index of refraction, thus requiring substantial porosity, e.g., over 80%, to lower their index to the level needed for a suitable AR coating on NOVA's silica lenses. This limits the composition to $SiO_2$ for all practical purposes.

In this report, formation of a graded index, wide spectrum $SiO_2$ AR coating on silica lenses is presented.

## 2. COATING SOLUTION PREPARATION

The $SiO_2$ film is deposited from a solution produced by hydrolysis of silicon ethoxide, $Si(OC_2H_5)_4$, in ethanol, $C_2H_5(OH)$.* Two major problems are immediately encountered in coating fused silica surfaces with hydrolyzed silanol solutions. First, such solutions do not readily wet fused silica surfaces, and second, $SiO_2$ films generally densify under normal heat treatment conditions. In our previous work, it was shown that these properties of the oxide polymer can be significantly altered by modifying its substructure.[23-24]

The reactions leading to the formation of polymer solutions from silicon ethoxide, $Si(OC_2H_5)_4$, can be presented as:

hydrolysis

$$[(RO)_3 \equiv Si - OR] + HOH \rightarrow [(RO)_3 \equiv Si - OH] + ROH \qquad (2)$$

polymerization

$$[\equiv Si - OH] + [RO - Si \equiv] \rightarrow [\equiv Si - O - Si \equiv] + ROH \qquad (3)$$

The second reaction arranges the various partially hydrolyzed species created by the first reaction into a polymer network. The skeleton of the main structural chains in these polymer molecules is analogous to the skeleton of fused silica and quartz. Heat treatment of these materials produces an organic-free oxide. Significant dissimilarities may occur, however, in the properties of the resultant oxide, such as melting point, viscosity, and sintering or densification

*See Appendix A for more information about these chemicals.

kinetics. These properties are closely related to the type and distribution of network bonds in the material, which are strongly affected by the polymerization method. For a given system, the parameters that introduce structural variations in the solution's polymer network may be listed as follows:

- $H_2O/Si(OR)_4$ ratio
- Molecular separation by dilution
- Electrolytic and catalytic effects
- Mixing method
- Reaction temperature

After a long and detailed investigation of the above parameters, individually and in combination, suitable solution formulas and preparation methods were developed for the AR coating for both spin and drain coating application techniques.

The solution which meets the needs of the present application for NOVA is produced under the following conditions:

- The $H_2O/Si(OC_2H_5)_4$ ratio is kept at 2.2 moles/mole (39.5 g of $H_2O$ per 208 g of $Si(OC_2H_5)_4$).
- During hydrolysis, the concentration of species is such that the solution contains 16 wt. % equivalent $SiO_2$ (e.g., 100 g of solution is made from approximately 55.5 g $Si(OC_2H_5)_4$, 10.5 g $H_2O$, and 35 g $C_2H_5(OH)$. This, when decomposed, gives 16 g $SiO_2$).
- Nitric acid at a concentration of 0.03 g (4.3 mg of 70% concentrated acid) per 100 g of the above solution is introduced as a catalyst for hydrolysis.

- Mixing is done under the following conditions: Water, alcohol, and acid are initially combined. Then $Si(OC_2H_5)_4$ is introduced rapidly to this mixture with vigorous stirring. (The order should not be reversed).

- The initial mixing is done at room temperature (20-25°C). The exothermic hydrolysis reaction raises the temperature of the mixture to about 45-48°C within 10-15 minutes. The mixture is then placed in an oven at 60°C for a period of 72 hours to allow the polymerization to take place. Refluxing may be done to reduce the required reaction time.

## 3. COATING DEPOSITION

### 3.1 Application of the Coating

Deposition of the coating from a solution can be done either by a spinning or a draining process. Spin application was used in the early development of the AR coating, where the substrates were 5 cm diameter quartz discs. In this method, cleaned substrates (see Appendix B for substrate preparation) were vacuum mounted on a variable speed chuck, the solution was deposited on the top surface, and the substrate was spun at a rate of 2500-5000 rpm [Fig. 1]. The polymer solution used for this method had a concentration of 15 wt. % equivalent $SiO_2$ and had been hydrolyzed using 2.0 moles water per mole alkoxide. The coated samples were then heat-treated and etched.

Since the spin coating technique was used only to expedite laboratory development, the transition from spin-coating to drain-coating had been anticipated from the beginning of this work. It was found, however, that this transition involved more than a mechanical transition; it required fundamental changes in the chemistry of the polymer solution as well as in the heat-treatment of the coating. The pore morphology created by the application of a given polymer on a substrate under drastically different speed and shear rates was quite different. To create a similar pore structure, drain coating required a solution which was formed under a 16 wt. % equivalent $SiO_2$ concentration and hydrolyzed by 2.2 moles of $H_2O$ (instead of 2.0) per mole of $Si(OC_2H_5)_4$.

### 3.2 Thickness Control of Coating

The thickness of the film applied from a solution depends on two groups of factors: those related to the solution and those related to the processing. In drain coating, the thickness, t, of the film can be represented by the equation:

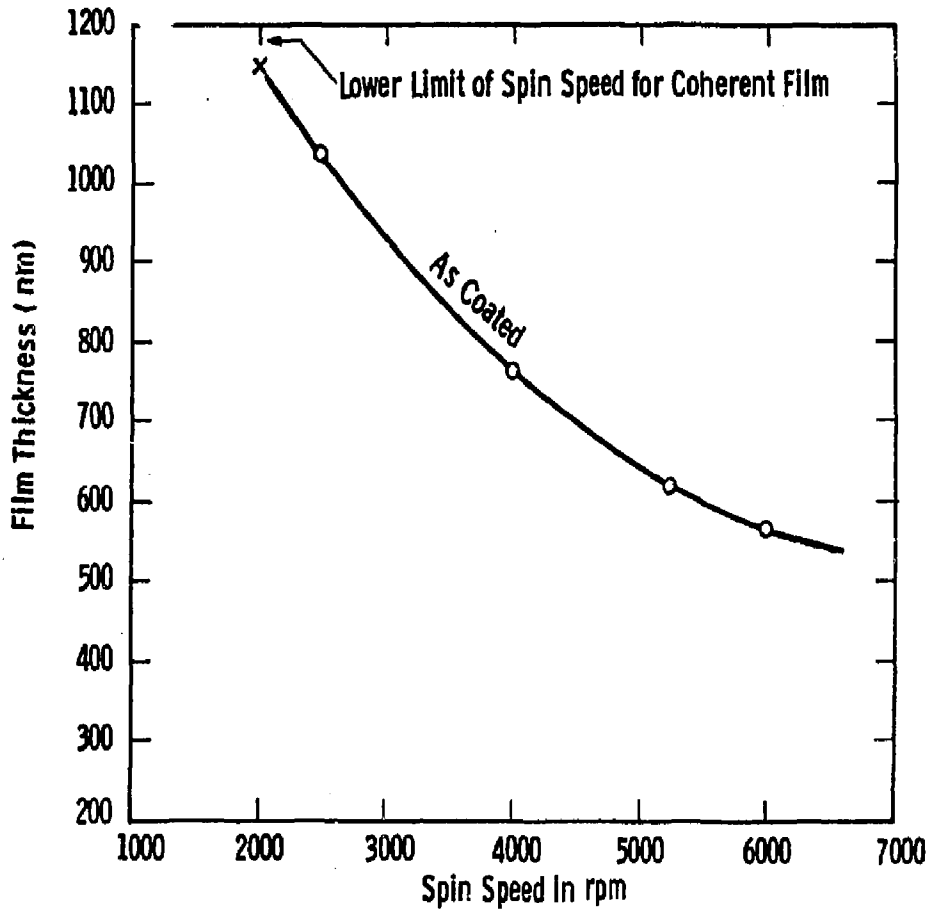


Figure 1 - Unfired coating thickness as a function of spin speed on 5-cm diameter optically polished silica discs.

$$t = \left( \frac{2 V_s \eta}{d \cdot g} \right)^{1/2} \qquad (4)$$

where $V_s$ is the pull or drain rate, $\eta$ is solution viscosity, d is the density of film and g is the gravitational constant. It must be noted that this equation is for undried films and, in our case, a drying factor must also be introduced. Wet films, even at optical thicknesses, are observed to run and drain when coated on vertical surfaces. A fast evaporation freezes the films and results in deposition of thicker coatings.[22]

Figure 1 shows coating thickness as a function of application rate in the spin coating of 5 cm diameter quartz discs. With the solution as described above, initial unfired coating thicknesses varying from approximately 500 nm to 1100 nm were obtained. Under these conditions, films thicker than 1000-1100 nm tend to craze upon heat treatment and are not acceptable. On the other hand, films thinner than ~600 nm become too thin after heat treatment to produce good anti-reflectivity in the desired spectral range.

Figure 2 shows coating thickness as a function of pull or drain rate in the drain coating process. (Note that the drain coating solution differs from the spin coating solution). As shown, in this case polymer orientation is such that the coating starts to show crazing at 700 nm. It must also be mentioned that the thickness dependence on drain rate, shown in Figure 2, will change somewhat with drying conditions.

As indicated in Equation 4, another factor that affects the coating thickness is the viscosity of the solution. Although the viscosity is set by the nature of the solution and its preparation to a value corresponding to ~2.8 cp, some external factors affect this. The main parameters that may change the solution viscosity are: aging, concentration change by evaporation of solvent, and temperature.

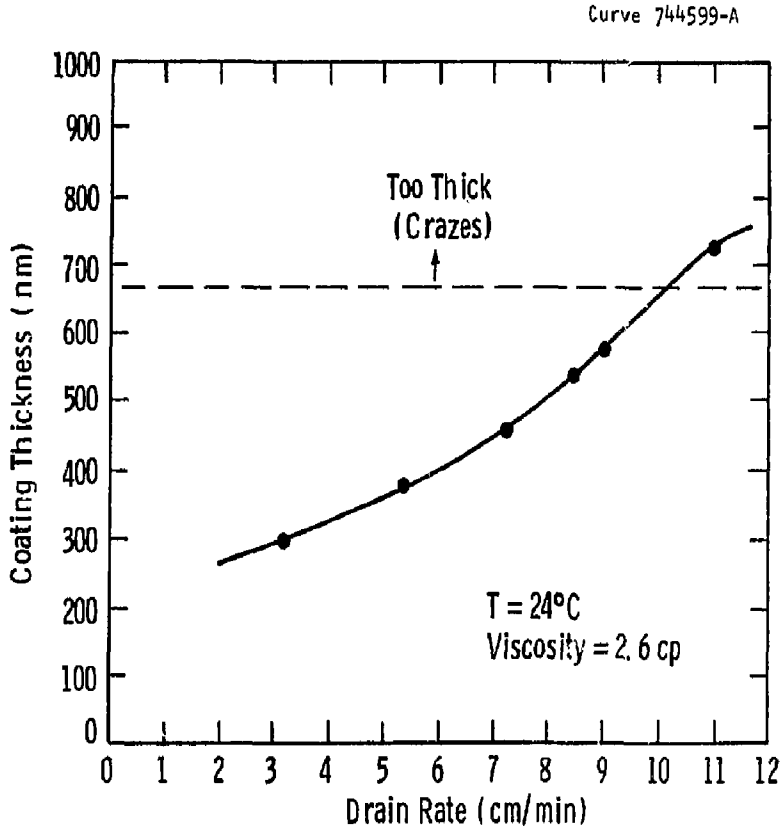


Figure 2 – Unfired coating thickness on optically polished silica as a function of solution drain rate.

The effect of aging of this solution was found to be insignificant. When the solution was initially prepared there was a slight drop in viscosity within 24 hrs. After that the viscosity at 21°C stabilized between 2.75 and 2.80 cp. This figure did not change observably in 30 days of aging. Even after 60 days there was only a slight increase in the viscosity from 2.8 cp to 3.0 cp. Thus it appears that the effect of aging on viscosity is not a significant factor within the first two months.

Figure 3 shows the effect of concentration change of the solution either by evaporation of ethyl alcohol or by dilution with it. A 1% change in the concentration, e.g., from 16% $SiO_2$ to 17%, requires evaporation of over 6% of the solution and causes only a 0.1 cp change in the viscosity. Thus concentration is also not thought to be a critical parameter.

However, among the three factors affecting viscosity, Figure 4 shows that temperature has the most significant effect on the viscosity of the solution. A 1°C difference in the temperature causes a variation in viscosity of approximately 0.1 cp. From Equation 4 it can be shown that this translates to about a 2% variation in coating thickness. At the thicknesses under discussion, this is about 5 nm. Although, as will be seen later, this is a small fraction within the AR thickness window, one must be aware of the effect of the temperature variation on thickness and take care that no significant temperature differences occur during coating application to ensure wavefront uniformity.

Ability to deposit very uniform thickness films by drain coating was demonstrated by coating 8" x 1.5" x 0.5" optically polished quartz plates. Figures 5 and 6 show interferometer and profilometer measurements of such films. If the substrate is not totally immersed in solution, a thinner coating is deposited on the upper 0.5-1.0 cm before the coating thickness stabilized at withdrawal rates of 5-10 cm/min.

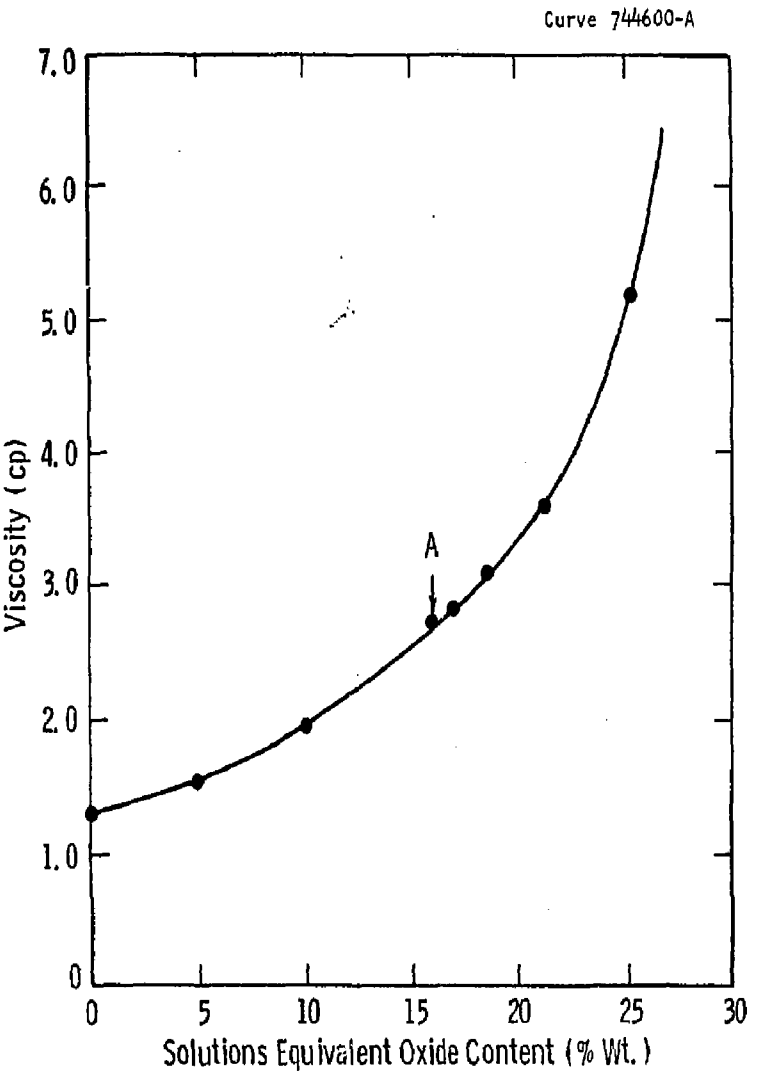


Figure 3 - Solution viscosity at 21°C as a function of equivalent oxide content. Point A corresponds to the drain-coating solution used in this work. Solutions with higher oxide contents are obtained by room-temperature evaporation of ethanol, while more dilute solutions are obtained by ethanol addition.

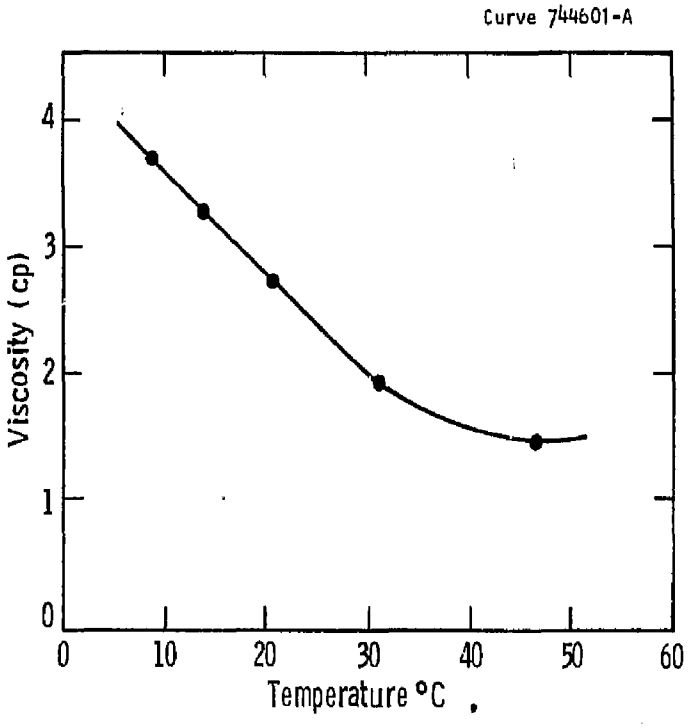


Figure 4 - Effect of temperature on the viscosity of the solution used for drain-coating.

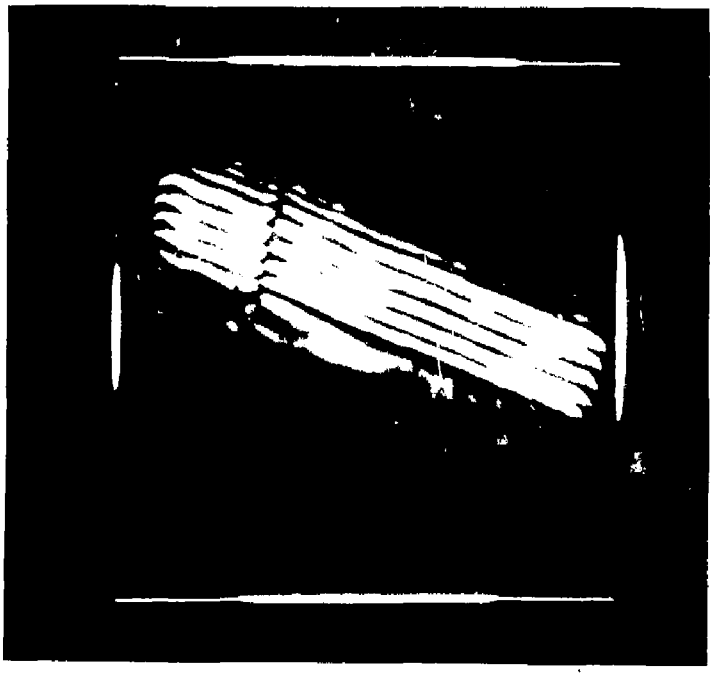

Figure 5 - Interferogram showing the coating uniformity of the $SiO_2$ polymer oxide on a 20 cm x 4 cm fused silica strip. The ridge shows where etching stops. The fringes are double pass transmission at 633 nm. Both sides are coated.

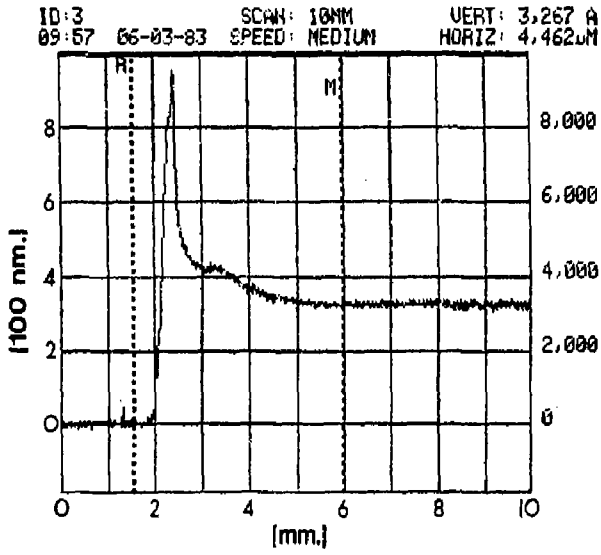


Figure 6 - Profile taken across the interface between the uncoated polished silica substrate and the coated region. This sample was prepared by masking the left (uncoated) area of the substrate with teflon tape during coating application. (The tape was removed before heat treatment). The ridge at the edge of the coating represents a meniscus created at the tape boundary. Such profiles illustrate both coating smoothness and thickness.

## 4. HEAT TREATMENT OF THE COATING

The applied film dries to a porous polymer layer having a general composition of $SiO_{2-(x+y/2)}(OH)_y(OR)_x$. OH and OR groups constitute ∿25% of the total weight and are bound at the terminating ends of the polymer molecules, whose main skeleton is similar to $SiO_2$ glass. OH groups make up ∿20% of the total polymer weight, while (OR) groups contribute perhaps 2-4%. Heat treatment is performed first to reduce the deposited coating to a pure organic-free oxide layer, $SiO_2$, and second to modify the original pore size. Temperatures of 450-500°C are required for the pyrolysis reaction:

$$SiO_{2-(x+y/2)}(OH)_x(OC_2H_5)_y + 6y\ O_2 \rightarrow SiO_2 + (5y+x/2)H_2O + 2y\ CO_2 \qquad (5)$$

Release of $C_2H_5$ groups is complex, and there is a possibility of carbon formation, which influences the laser damage resistance of the coating. For example, chemical bonds which rupture in the temperature range of 150-200°C result in deposition of carbon.[25] This can generally be avoided by heating the silanol polymer reasonably fast between the temperatures of 150 and 200°C, e.g., 7-10°C/min. (see Figure 8 in Reference 25.) The chance of carbon formation can also be reduced by keeping the film thickness as low as allowed within the optical constraints (see Section 5).

Through complete pyrolysis of the material, a porous $SiO_2$ film is formed. The porosity is continuous, that is, interconnected, and open, with a configuration somewhat similar to closely spaced worm holes (see Figure 7). The percent porosity and pore size depend to a degree on the preparation method, but the pyrolyzed material is normally about 55% porous with pore diameters of 2-3 nm. As discussed in Section 5, grading of this porosity to a depth of one quarter of the longest wavelength is accompanied by enlargement of the surface pores

Figure 7 - Electron micrograph of a fractured surface replica of bulk silica glass obtained by pyrolysis of the drain-coating solution shows the pore morphology.

which is sufficient to cause the pores to join, leading to scattering at the shorter wavelengths, e.g., 350 nm. For this reason the initial pore size must be reduced below a critical size without causing pore closure (see Figure 8).

When pore size tailoring by heat treatment is performed, certain very important considerations come into play. An awareness of these factors and control over their effects are necessary for the formation of a pore morphology suitable for index grading. These factors are:

A. The initial hydrolysis conditions of the precursor solution, especially the $H_2O/Si(OC_2H_5)_4$ ratio and molecular spacing, i.e., concentration, have a paramount influence on the densification properties of the deposited $SiO_2$ layer.[23,24]

B. The method of coating deposition, i.e., whether spin or drain coated, again has profound effect on the densification properties.

C. The effect of humidity during drying of the coating is important. High humidity conditions during the drying promote densification to a degree that precludes tailoring of the pore morphology.

D. Densification of the coating is not a linear function of temperature. There are temperature regimes in which the polymer coating shows accelerated sintering and temperature regimes where very little densification occurs (see Figure 9).

The effect of hydrolysis, e.g., water/alkoxide ratio, on the sintering properties of oxide polymers was previously known.[23, 24] But the effect of the deposition method was surprising. For example, the solutions developed by spin coating required 16 hrs of heat treatment at 600°C to produce a suitable pore size for index gradation. When the same solution was deposited by draining, the coating densified during heat treatment at much lower temperatures. Investigations using a

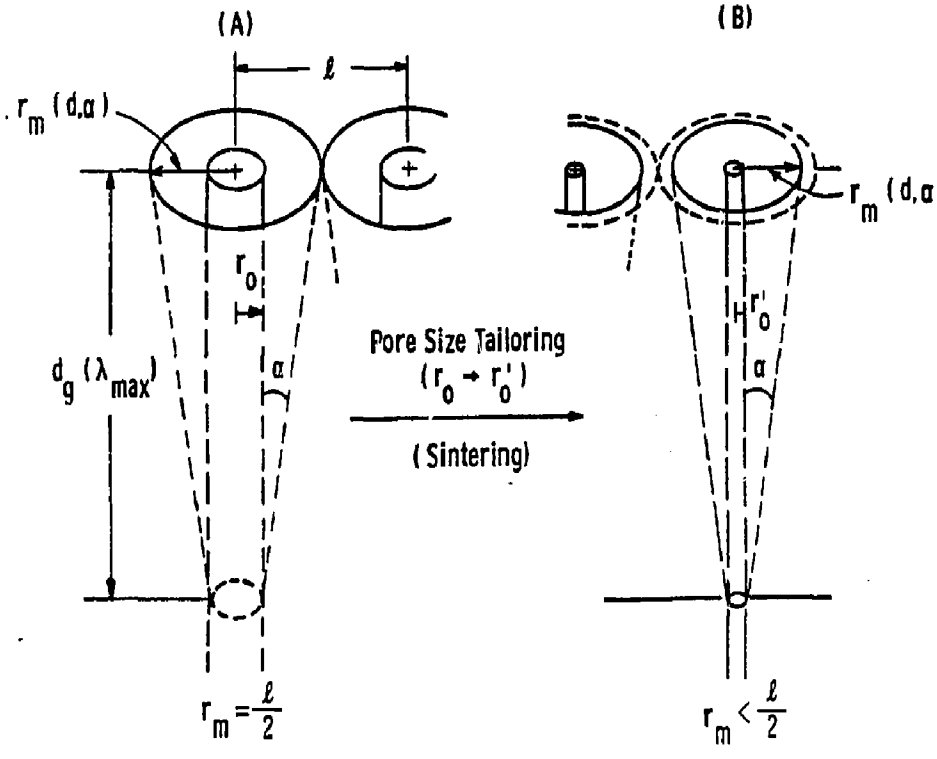


Figure 8 - Gradation of the initial pores (shown Schematically as cylinders) by etching to a depth $d_g$ may cause surface pore enlargement that causes joining of pores (A). This is prevented by shrinking the initial pore diameter $r_o$ to $r_o'$ by a heat treatment before grading (B).

Curve 739974-A

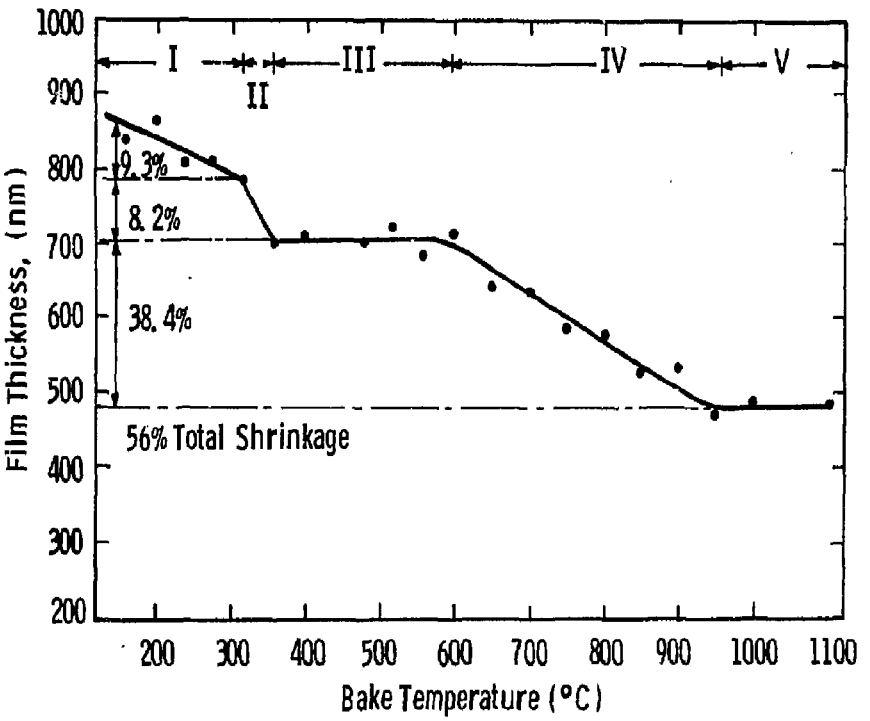


Figure 9 - Change in the thickness of a ∿900 nm $SiO_2$ film deposited on fused silica as it proceeds through sintering.

temperature-time matrix showed that there was no suitable heat treatment regime which would give a suitable pore morphology by drain coating from this solution. The reason for this is thought to be that film deposition by drain coating at several cm/min allows for polymer orientation and alignment on the surface, a situation which is drastically different from spin coating, where deposition occurs at several thousand rpm under fast drying conditions. The gentle linear motion of drain coating aligns the polymer units into a denser configuration. Therefore, it was clear that another type of polymer structure needed to be developed. Further study led to the development of another solution, which has a higher $H_2O/Si(OC_2H_5)_4$ ratio and is higher in $SiO_2$ concentration. This solution required a heat treatment 100°C below that used for spin-coated films, and the optimum heating time was much shorter, e.g., 485°C, for 4 hours rather than 585°C for 16 hours.

Figure 9 shows that, when a coating is completely densified, its thickness is reduced by 56%, which means that it was initially 56% porous. Figure 10 shows that the heat-treatment designed for the spin-applied coating, i.e, 585°C for 16 hours, results in a 37-40% thickness shrinkage. This implies elimination of 2/3 of the pore space. Calculations show that this corresponds to a shrinkage of approximately 70% in the pore diameter, reducing the original pore size to less than 1 nm (perhaps as low as 0.6 - 0.7 nm). Only such a small initial pore size appears to be suitable for index grading without causing scattering at the 350 nm wavelength. The effect of this heat treatment on the index of refraction of the coating is schematically represented in Figure 11. The initial coating before firing might be expected to have a lower index, but it is actually $\sim$1.38 due to the presence of organics and hydroxyl groups (A);when pyrolyzed at 500°C, it goes through an intermediate stage (B);holding the film at that temperature long enough brings it to the final state (C). In this final state prior to etching, the $SiO_2$ film has an index of refraction $\sim$1.40 and a porosity of $\sim$20% made up of pores whose diameter is less than 1 nm. In the case of drain coating, the heat treatment of the coating to produce a suitable pore size and matrix was shown to be significantly different. A 4-hour heat treatment at 485-500°C was found to be sufficient.

Curve 740672-A

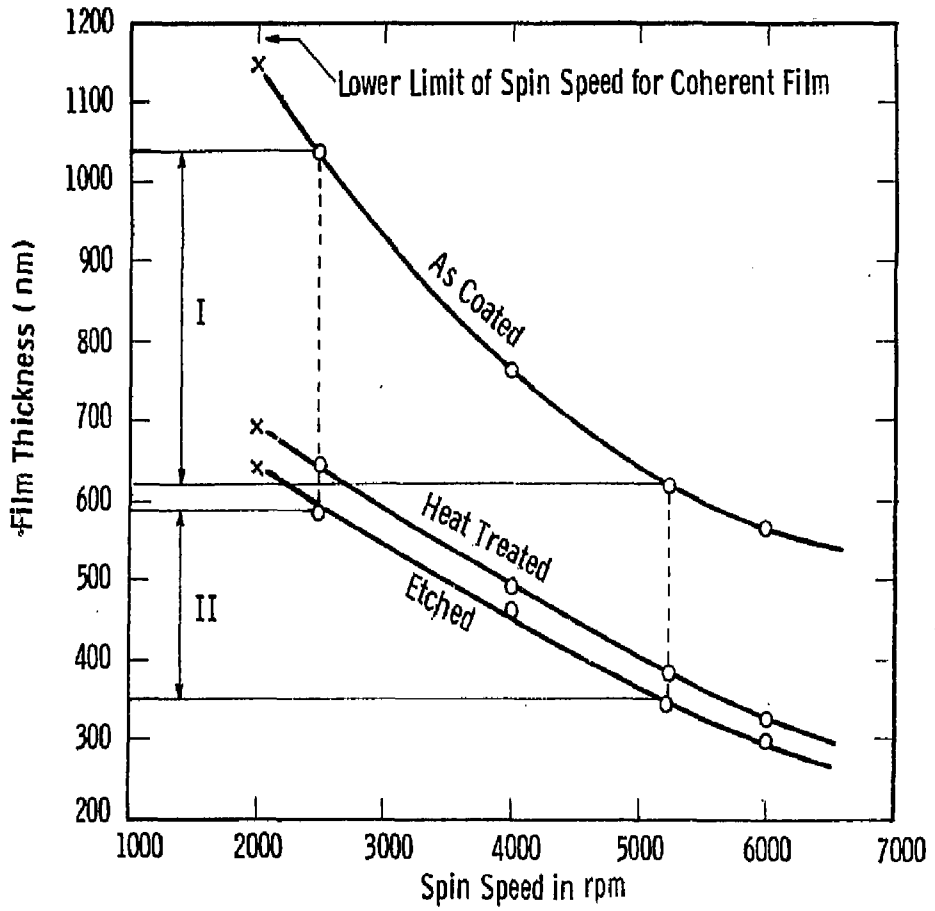


Figure 10 - Film thickness decreases as spin application speed is increased and is further reduced during heat treatment and etching. Area I designates the unfired film thickness range which, after firing and etching, translates to Area II. Only films falling within Area II show acceptable AR characteristics.

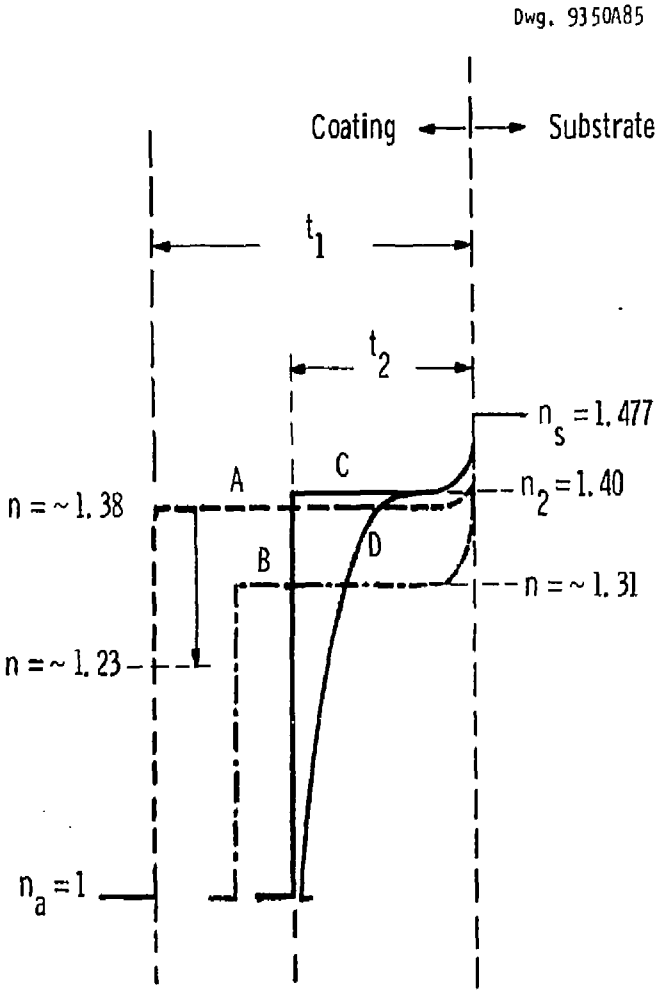


Figure 11 - Various stages in coating treatment

A. As-coated, unfired film. Refractive index is ∿1.38 due to the presence of OR and OH groups. The pure $SiO_2$ analogue would be ∿1.23.
B. Pyrolyzed film. (porosity ∿40%; pore diameter ≲2 nm)
C. Film with tailored pores. (porosity ≲19%; pore diameter ≲1 nm)
D. Film with graded pores.

It was also determined that the process is very flexible as to the heating rate and holding temperature. Heat-up times of 30 minutes to 6 hours to get to ∿500°C appeared to be acceptable, i.e., ∿16°C/min. to ∿1°C/min. In addition, final hold temperatures as high as 600°C did not lead to excessive film densification, as long as the coating had been dried in an atmosphere of low humidity. A heating rate of 4°C/min up to 500°C and holding the sample 4 hours at that temperature was selected as an appropriate schedule for the large NOVA lenses. This would involve a heat treatment totaling ∿6 hrs, not including the cool-down time. In one experiment, samples held at a temperature of 510°C for 2, 3, and 4 hours all had similar spectral transmission profiles, indicating that the time of holding after 2 hours is rather flexible.

Figure 12 shows the effect of such a heat treatment on the thickness of the film depositd by drain coating. One noteworthy feature of the curve is that the shrinkages causes by the heat treatment of drain coated films is much smaller than for spin coated ones (∿23% vs 40%, for example). Also, crazing of the film occurs at a lower thickness than for the spin coating (∿700 nm vs ∿1000 nm). This phenomenon is thought to be due to deposition of the denser films with drain coating by more efficient polymer orientation and alignment, as mentioned previously.

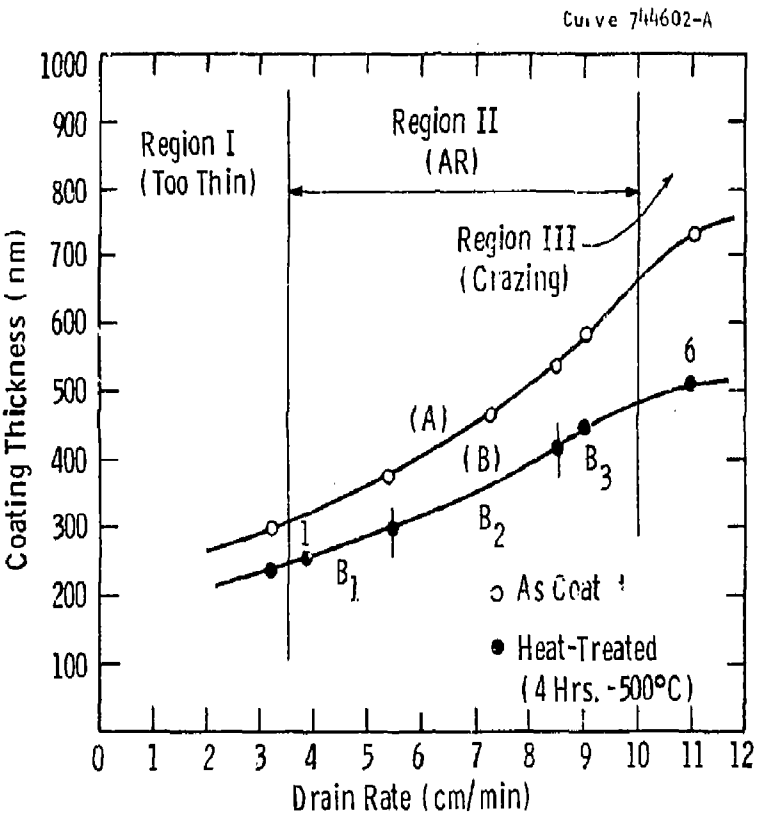


Figure 12 - Thickness of a $SiO_2$ coating deposited on optically polished fused silica as a function of application rate using the drain coating technique. (A) is for unfired films, and (B) is for heat-treated films. Only films within region II show acceptable AR characteristics.

## 5. INDEX GRADATION AND OPTICAL PROPERTIES

The subject of graded films and the mathematical treatment of the optical response that might be expected from such films have been addressed in the literature.[16, 27-30] A schematic representation of such a graded film is shown in Figure 13.

In the initial stages of this project, there was no difficulty in producing an antireflective coating with less than 0.5% reflectivity over the entire 350 nm to 1100 nm spectral range. However, transmission curves of the same films showed precipitous drops in the transmission toward the UV, so that the transmission was often as low as 70-80% at 350 nm (see Figure 14). This problem of scattering was addressed by first shrinking the pore size through heat treatment and second by formulating an etchant that creates a gradation in pore size one-quarter wavelength deep without enlarging any of the pores to a size where they scatter. (Scattering goes up with the sixth power of the pore size.) One can tell, through the behavior of spectral transmission curves as a function of etching time, whether scattering is due to incomplete sintering, too much etching, or improper polymer formation. Etching required use of a very dilute etching agent. The table below shows the concentration of HF and corresponding time required to induce the porosity grading needed for a wide spectrum AR coating at room temperature (25°C).

Table 1

| Concentration* (% wt HF) | (48% HF) | Time to Produce AR Film |
|---|---|---|
| 0.048 | 0.100 | ∿9 min |
| 0.036 | 0.075 | ∿18 min |
| 0.024 | 0.050 | ∿38 min |

*A 48% solution was diluted with distilled $H_2O$. (For example, to produce the first solution, 1.0 g of 48% HF was added into 999.0 g $H_2O$.)

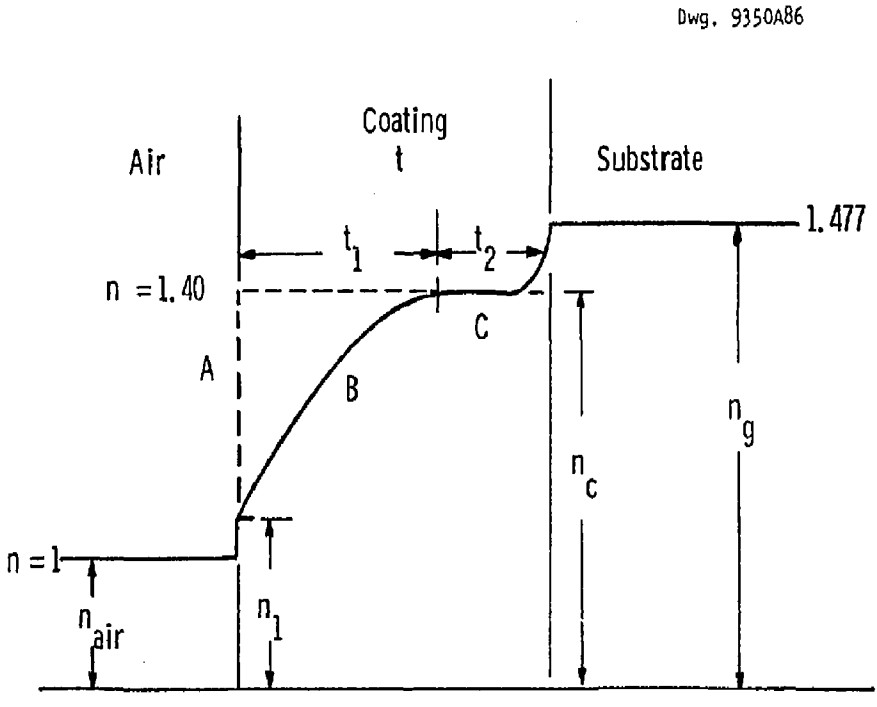


Figure 13 - Schematic representation of a graded index film on fused silica at 350 nm.

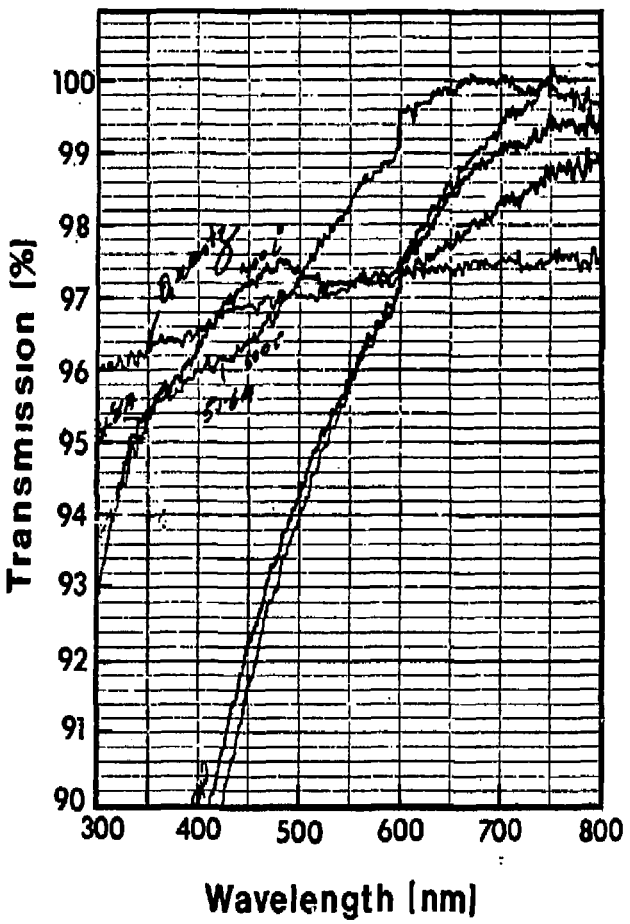


Figure 14 - Films of low reflectivity may show very poor transmission at short wavelengths due to scattering by the pores.

It appears that all of the above treatments produce equivalent AR properties. In most of our experiments, we have used the 0.036% HF concentration with 18 minutes of etching at room temperature.

The microstructure of the film graded under these conditions was investigated using SEM and TEM. Transmission electron microscopy was more successful. In this method, the AR coating was formed on a fused silica sample, the coating surface was covered with evaporated aluminum, the sample was embedded in epoxy, and finally, the whole aggregate was sliced vertically and thinned by ion milling.

Figure 15 shows a typical transmission electron micrograph of the graded-porosity coating. In this particular sample, the coating is ∿500 nm thick, and gradation of the pore size in the first 100-150 nm is clearly shown, as well as the porous substructure of the ungraded film. It appears that the pore size of the unetched film is of the order of ∿1 nm and, when etched, the larger surface pores attain a size of 3-4 nm.

Figure 16 shows a typical spectral transmission curve for a spin-applied AR coating. Spin applied coatings (and that particular solution) tended to produce transmission curves which sloped down toward the UV. Although readings close to 100% were not unusual between 1100 and 800 nm, the transmission gradually dropped to about ∿98% around 300 nm.

On the other hand, the coating deposited by draining often showed an increasing transmission toward the UV. It is also possible to produce flattened curves where the transmission stays over 99.5% through the entire 800 to 350 nm region (See Figure 17).

The effect of thickness on the AR performance of the film was investigated by coating a 8" x 1.5" x 0.5" fused silica slab at a liquid draining rate which varied continuously from 3 cm/min to 12 cm/min. The sample was then heat-treated. The thickness of the film after heat treatment varied from ∿200 nm for the 3 cm/min drain rate to ∿500 nm for the ∿10 cm/min rate. After etching the antireflective region extended over a thickness range of 250 nm to 500 nm. This zone was shown in Figure 12

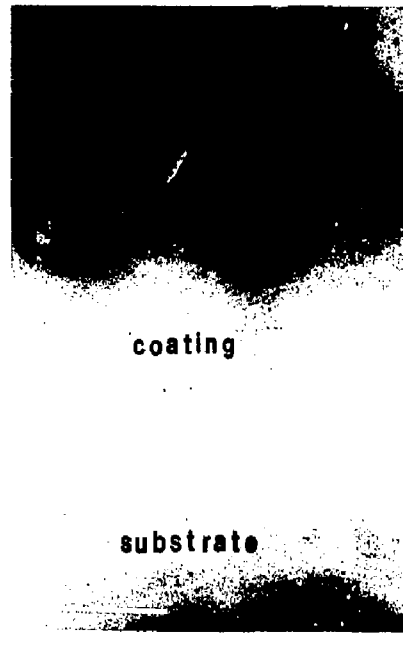


Figure 15 - Transmission electron micrograph showing the cross section of a coating with graded porosity. An evaporated aluminum layer, shown here as a dark band, was applied over the coating for spatial reference. Above that is the epoxy mounting material.

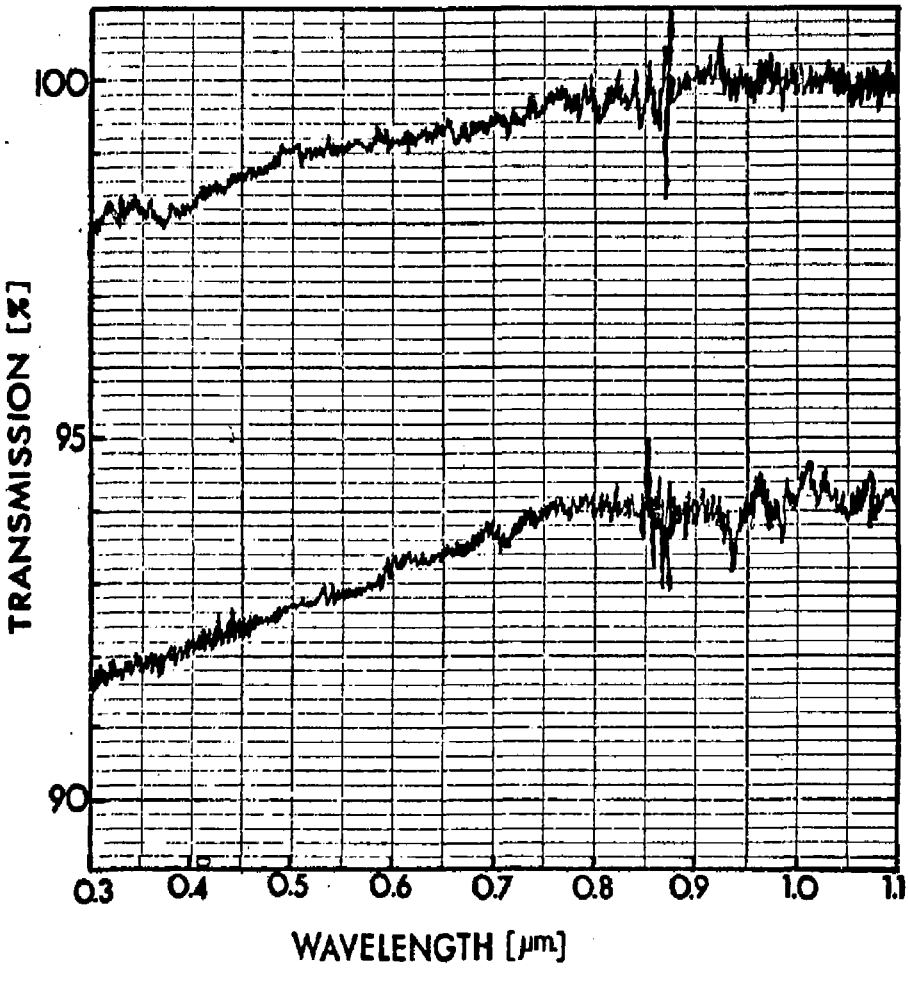


Figure 16 - Spectral transmission curve of a fused silica substrate with both surfaces AR coated with the spin-applied coating (upper curve). With this application technique, the transmission tends to deteriorate somewhat toward short wavelengths. The lower curve is for uncoated fused silica.

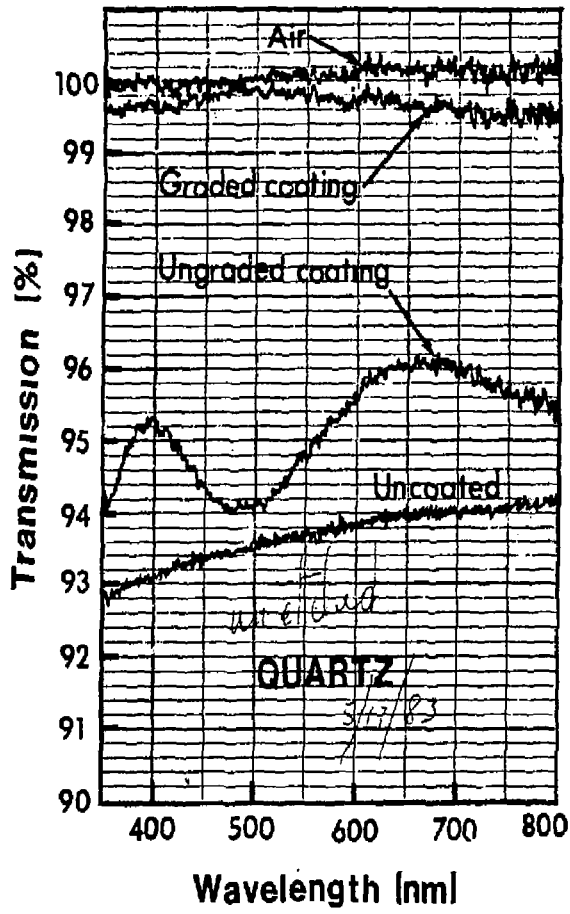


Figure 17 - Spectral transmission curves for a drain-coated fused silica substrate, before and after gradation of the pores. Note that there is no deterioration in ultraviolet transmission of the graded coating curve. Reference curves for silica and for air are also included.

as Region II. The AR region had a bluer hue toward extremes $B_1$ and $B_3$, and its central area, $B_2$, appeared grayish or slightly yellow. Spectral transmission curves were obtained at 7 points corresponding to various known thicknesses along the sample. Two of these curves are shown in Figure 18. Point #6 (top curve in Fig. 18) has a thickness of ∿500 nm, and point #1 (bottom curve) has a thickness of ∿250 nm. As shown, the 250 nm thickness provides an AR coating which is as good or better than the 500 nm thickness over the entire spectrum. This suggests that the thickness window is wide and flexible but, since the thinner coating is expected co give a better laser damage threshold, one should deposit thinner coatings than previously used, e.g., in the range of 3-5 cm/min drain rates.

Figure 18 also demonstrates that these AR coated samples show as much as 98.8% transmission even at the 250 nm wavelength. Of course, at these low wavelengths, absorption by the $SiO_2$ substrate begins to influence the transmission. It is also of interest to note that, unlike the many other porous coatings, spectral transmission curves of these samples showed very little change even after the samples were allowed to stand for months in the laboratory, where the atmosphere has a relative humidity of 50-70%.

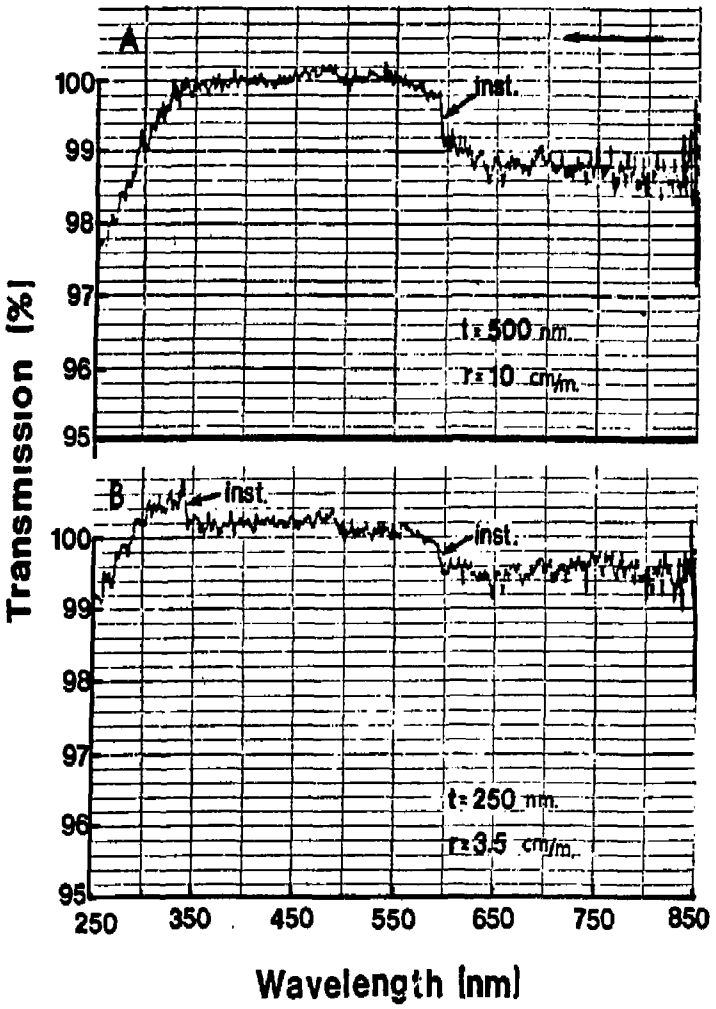


Figure 18 - Spectral transmission curves of drain-coated fused silica substrates where the fired coating thickness is 500 nm (A) and 250 nm (B). The drain rates used to achieve these thicknesses are also given. Shifts in the transmission curves occur where there is a detector change in the instrument. (Perkin Elmer model 350).

## 6. LASER DAMAGE INVESTIGATIONS AT 3ω

Laser-induced damage to AR coatings is often the limiting factor in operation of high power lasers.[19, 31] The mechanisms which cause laser damage in optical materials are numerous and have been reviewed by other authors.[32-37] These causes can be divided intially into two general categories. The first is intrinsic non-linear processes which are determined by the nature of the material and caused by such phenomena as two photon absorption or avalanche breakdown. This category determines the theoretical upper limit of the irradiation and is not of a particular concern here; $SiO_2$ has a sufficiently high intrinsic damage threshold for the intended purpose, even though 3ω is getting close to the UV absorption edge of $SiO_2$. The second category of laser damage is caused by included particulates as well as chemical variations and inhomogenieties which lead to localized absorption; this determines the actual practical irradiation level. This second category of laser damage essentially governed the threshold values in this work and therefore was a prime subject of investigation.

When damage occurs due to inhomogenieties, the damage threshold has been shown to depend significantly on pulse duration[35,36] and laser wavelength.[38,39] Short pulses can more easily damage small inclusions. More significantly, as the laser wavelength is decreased, a new spectrum of absorption sites, previously too small to interact, start to dominate the damage mechanism.

In this work the damage measurements were done exclusively at 3ω (350 nm). The coatings were applied to 5 cm diameter optically polished fused silica discs provided by LLNL using both spin and drain coating application methods. The damage measurements were done at LLNL under the supervision of Dave Milam. In excess of one hundred samples were tested. Damaged sites were later examined by optical microscopy as well as SEM.

In the early part of the work, a great emphasis was placed on filtration of the coating solution (see Appendix C), since it was thought that inclusion of particulates in the solution was the main cause of laser damage. However, it soon became apparent that this was not a dominating factor, although it may have been a contributing factor. First, some laser damage resistant coatings were produced without solution filtration, and second, the density of the damage sites appeared to far exceed what one might reasonably expect from a population of particulate inclusions. Furthermore, when a group of substrates was coated in succession with the same solution and heat treated together, they exhibited entirely different damage behavior. This is illustrated, for example, in the "84 series" shown in Figure 19. Sample 84-1 (A) exhibits few laser damage sites at a 9.6 $j/cm^2$ fluence, compared to Sample 84-7 (B), where the damage sites cover almost the entire surface at a fluence of only 4.1 $j/cm^2$. Samples 84-8 and 84-9 (shown as C and D) in Figure 19 exhibit a clustering of damage sites which would be uncharacteristic of particulate-induced damage, since one would expect a more homogeneous distribution of subcolloidal particulates in a liquid coating solution.

Optical observation of laser damage sites revealed one other very significant piece of data: that almost all laser damage sites were originating from the same depth, which corresponded to the coating thickness. This indicated that the substrate surface or the substrate/coating interface was playing a very significant if not a dominating role in laser damage. Based on this observation various substrate surface cleaning methods were investigated (see Appendix B). These included both chemical and mechanical techniques.

The first group of samples (142-1 through 142-4) showing encouraging damage thresholds had been made from substrates which were cleaned using an automated scrubbing technique used in the semiconductor processing industry (described in Appendix B). The thresholds of this group ranged from 3.5 to 5 $j/cm^2$. (See Table 2.) However, further experiments showed that scrubbing of the substrate surfaces in no way guaranteed a reproducibly high damage threshold. Large numbers of

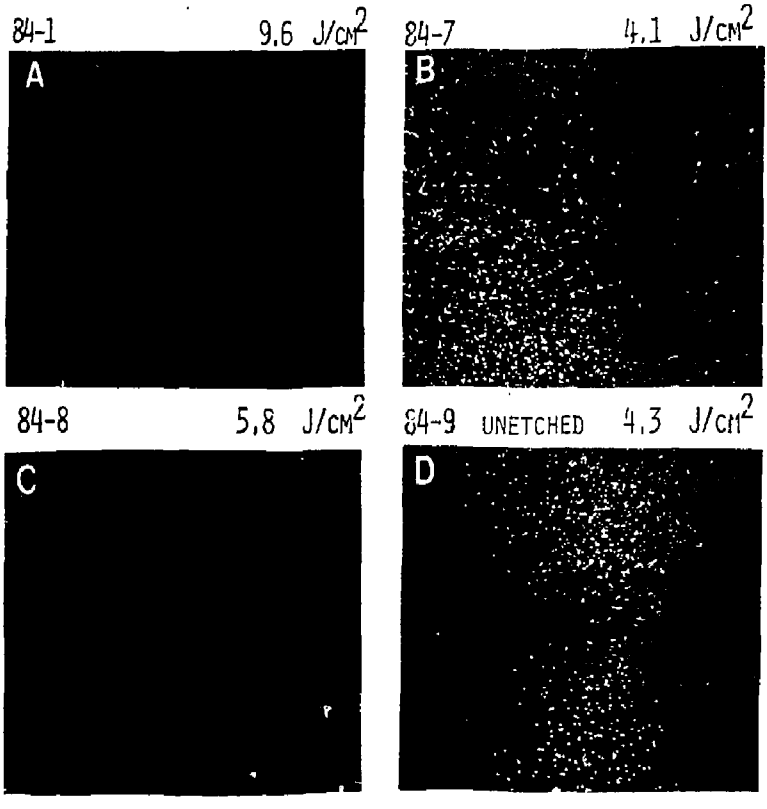


*Figure 19 - Laser damage site density and pattern of four samples which were processed together. Note that the damage characteristics vary from low density, high threshold (A) to high density, moderate threshold (B). Also, note that the damage site distribution may be uneven (C and D).*

TABLE 2

LASER DAMAGE THRESHOLDS OF SPIN COATED SAMPLES* AT 355 nm WITH A 0.6 ns PULSE

| (W) Sample No. | $SiO_2$ Disk No.(#) | L.L. Test | Damage Threshold (†) ($j/cm^2$) |
|---|---|---|---|
| 142-1 | 3372 | L-180 | 3.3 ± 0.5 |
| 142-2 | 3368 | L-181 | 4.3 ± 0.6 |
| 142-3 | 3378 | L-182 | 5.0 ± 0.7 |
| 142-4 | 3391 | L-183 | 4.6 ± 0.7 |
| 142-5 | 3411 | L-184 | <2 |
| 142-6 | 3415 | Not Tested | Not Tested |
| 142-7 | 3416 | L-185 | 4.3 ± 0.6 |

(†) As observed by Nomarski Microscopy.

(*) Spin coated on in-house polished 5 cm silica discs at 4000 rpm (142-1 at 3000 rpm), fired at 585°C for 16 hrs in a $O_2/N_2$ atmosphere, and porosity graded.

(#) These discs had originally been polished and numbered by Zygo but were re-polished by Westinghouse before these samples were coated.

samples were prepared to test the effect of variations in substrate cleaning, coating deposition method, heat treatment, etching, etc. Results were generally disappointing, as shown in Table 3. It was becoming clear that laser damage in these samples was being induced by a number of factors, some of which were still unknown. To do meaningful studies it was necessary not only to identify these factors but also to separate and isolate their overlapping effects.

The multiplicity of the sources of laser damage is also indicated by Figures 20 and 21. Figure 21 shows that the activation energy for the origination of new damage sites was strongly sample-dependent. The reason for this may be related either to the size of the absorption sites,[32] or to differences in the nature of the absorption sites. Indeed there are several distinctly different types of damage morphology indicated by visual observations of hundreds of damage sites. Four types of damage morphology often encountered in these samples are shown in Figure 21.

A list of theoretically possible sources of laser damage was prepared and is shown in Table 4, where these sources are cataloged under five major headings. These are:

- Substrate
- Surface Preparation (polishing, cleaning)
- Solution
- Heat Treatment
- Etching.

Some of the potential laser damage sources shown in Table 4 can be readily eliminated. For example, the fact that we had already achieved acceptably high laser damage in some samples would rule out such factors as intrinsic unsuitability of the solution or detrimental effects of $HNO_3$. The source(s) of damage obviously varied from sample to sample, but those factors which were constant among samples could be ruled out as the dominating factors.

Dwg. 5608C78

TABLE 3
WESTINGHOUSE POLYMER OXIDE AR COATINGS
TESTED AT 355 nm WITH 0.6 ns PULSES

| Batch; Date | Disc # | Test #L- | Westinghouse I.D. # | Substrate Polished by | Cleaning | Coating [4] | Etching [5] | Cosmetic Appearance | Damage Growth Rate vs Fluence | Threshold ($J/cm^2$) |
|---|---|---|---|---|---|---|---|---|---|---|
| #6 Feb. | 1382 | 310 | 74-1 | 7940 Unertl | Westinghouse [2] | Westinghouse Spin | Etched 18 min, 0.075 HF | Not Noted; Clean in Microscope | Large Massive at < 1.5 $J/cm^2$ | 1.1 ± 0.3 |
| | 3452 | 311 | 74-3 | Suprasil 2 Zygo | Westinghouse [2] | Westinghouse Spin | Etched 18 min, 0.075 HF | Dirty | No Data Above Threshold Slight Damage at 2.6 $J/cm^2$ | 2.3 ± 0.3 |
| #7 Mar. | 3448 | 318 | 84-1 | Suprasil 2 Zygo | Westinghouse [1] | Westinghouse Spin | Etched Half | Clean With Isolated Artifacts | Low Slight Damage at 4.7 $J/cm^2$ | 2.7 ± 0.8 |
| | 3448 | 320 | 84-1 | Suprasil 2 Zygo | Westinghouse [1] | Westinghouse Spin | Unetched Half | Clean | High Massive Damage at 5.7 $J/cm^2$ | 2.8 ± 0.5 |
| | 3467 | 321 | 84-2 | Suprasil Zygo | Westinghouse [1] | Westinghouse Spin | Etched Half | Dirty | Low Slight Damage at 5.0 $J/cm^2$ | 2.9 ± 0.5 |
| | 3467 | 322 | 84-2 | Suprasil 2 Zygo | Westinghouse [1] | Westinghouse Spin | Etched Half & Half Hr, Aqua Regia | Dirty | Moderate Slight Damage at 4.1 $J/cm^2$ | < 2.5 |
| | 1383 | 315 | 84-3 (46) | 7940 Unertl | Westinghouse [1] | Westinghouse Spin | Etched | Foggy; Many Microscopic Pits & Scratches | Moderate Moderate Damage at 6.7 $J/cm^2$ | 2.4 ± 0.4 |
| | 1384 | 317 | 84-4 (41) | 7940 Unertl | Westinghouse [2] | Westinghouse Spin | Etched Fired in $O_2$ | Clean to Eye; Some Microscopic Pits & Scratches | Large Moderate Damage at 3.5 $J/cm^2$ | < 2.2 |
| | 1385 | 324 | 84-5 (44) | 7940 Unertl | Westinghouse [2] | LLNL Dip | Not Etched | Totally Crazed; Much Debris | Large Much Damage at 4.0 $J/cm^2$ | 2.2 ± 0.3 |
| | 3517 | 316 | 84-7 | Suprasil 2 Zygo | LLNL [3] | LLNL Dip | Etched | Some Crazing & Isolated Artifacts | Large Massive Damage at 2.9 $J/cm^2$ | < 2.2 |
| | 3517 | 323 | 84-7 | Suprasil 2 Zygo | LLNL [3] | LLNL Dip | Etched; Cleaned Before Test | Some Crazing & Isolated Artifacts | Large Moderate Damage at 2.3 $J/cm^2$ | 1.8 ± 0.3 |
| | 3518 | 319 | 84-8 | Suprasil 2 Zygo | LLNL [3] | LLNL Dip | Etched | Some Crazing | Large Massive Damage at 5.8 $J/cm^2$ | 2.1 ± 0.3 |
| | 3519 | 325 | 84-9 | Suprasil 2 Zygo | LLNL [3] | LLNL Dip | Not Etched | Some Crazing | Large Massive Damage at 3.8 $J/cm^2$ | 2.2 ± 0.3 |

[1] Ultrasonic Agitation in Hot "Micro"/$H_2O$; Immersed in $H_2SO_4/H_2O_2$; Nylon Scrub

[2] Ultrasonic Agitation in Hot "Micro"/$H_2O$; Immersed in $H_2SO_4/H_2O_2$; No Nylon Scrub, Propanol Cleaning

[3] Tincture [illegible] Green Soap; Distilled Water Rinse; 5 Min. Spin Dry

[4] 0.02 μm Filtered Solution; > 500°C Bake

[5] 0.075 % HF Etch for 18 Minutes

Curve 7451 24-A

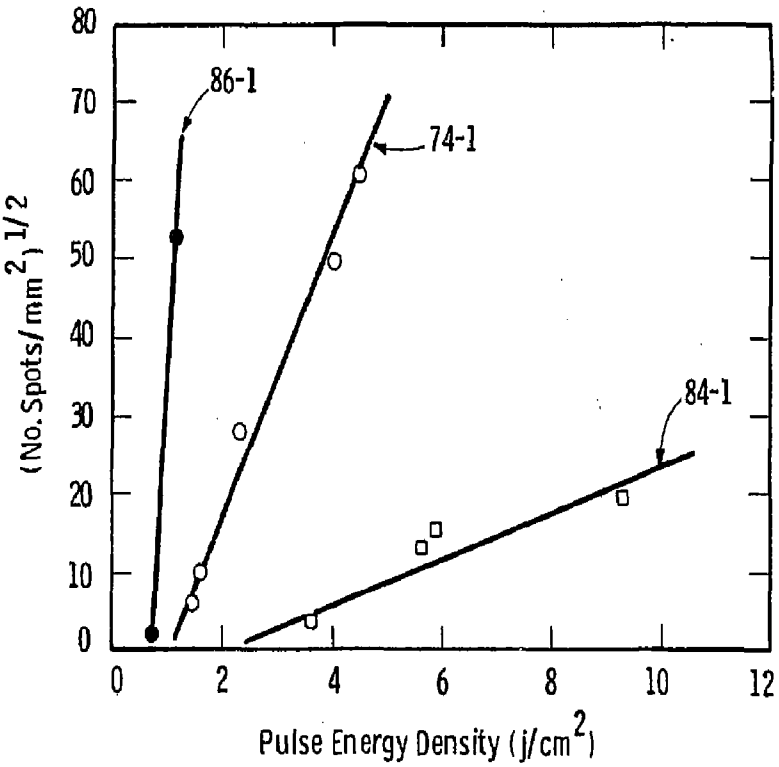


Figure 20 - Number of laser damage pits vs pulse energy density.

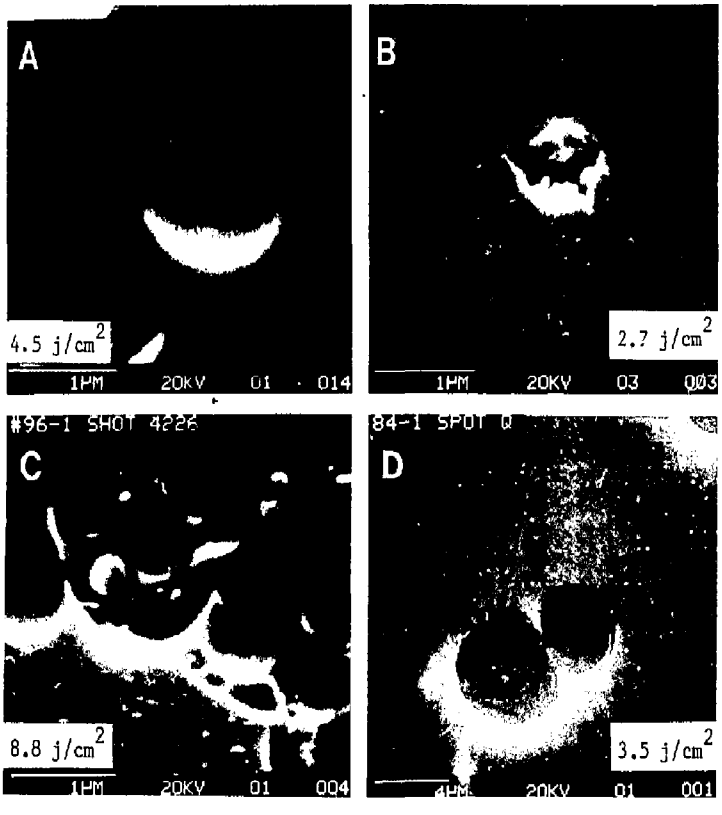


Figure 21 - Scanning electron micrographs of some typical laser damage morphologies observed in $SiO_2$ polymer oxide coatings.

TABLE 4

LIST OF POTENTIAL SOURCES OF LASER DAMAGE

| | Possible Damage Source | Possible Solution |
|---|---|---|
| Substrate $SiO_2$ | Impurities | High purity material |
| Surface Preparation | | |
| A) Polishing: | o Partly embedded particles | Scrubbing, chemically dissolving |
| | o Fused particles | Chemically dissolving |
| | o Damaged surface | Annealing |
| B) Cleaning: | o Introduction of particles | Clean practices |
| | o Damaging surface | Annealing |
| Coating Solution | o Particulates in solution | Distillation or precursors filtering |
| | o $HNO_3$ is a problem | Use less, replace |
| | o Aging, polymer growth | Less aging, less heat treatment, etc. |
| | o Solution is intrinsically unsuitable | None |
| Heat-Treatment | o Cracks originate | Thinner coatings |
| | o Organics left | Change heat treatment conditions. Change solution. |
| | o Carbon forms | Change hydrolysis, polymerization, aging, precursor Si material, or heat treatment conditions. Dissolve or react organic or carbonaceous components. |
| | o Introduction of particles | Clean practices |
| | o Surface damage | Change etch conditions |

The presence of cracks or crazing in the coating also does not appear to cause laser damage. Cracks in these coatings are generally caused by one of two mechanisms. One occurs when the deposited coating is too thick, e.g., thicker than 500 - 600 nm (see Figures 10 and 12). We have never observed any laser damage associated with this type of crazing. The other happens when an included contaminating particle generates a crack. Such a crack is shown in Figure 22-A, where a $\sim$ 200 μm long crack in the coating was generated by a small particle identified by EDAX as magnesium silicate (lower left end of the crack). As shown in this figure, no laser damage sites are associated with this crack, whereas the particle exploded and evaporated under $\sim$ 4j/cm$^2$ fluence. This damage morphology is shown in 22-B.

On the other hand, scratches on the substrate may be very detrimental. For example, a sample exhibiting a very high laser damage threshold, i.e., 8.8 j/cm$^2$, contained a thin streak of intense damage running across the laser-irradiated spot as shown in Figure 23. Further examination revealed that the damage streak coincided with a linear feature on the fused silica which happened to cross the irradiated area. Basically, the feature looked like a polishing defect such as an incompletely removed scratch, which extended some distance beyond the boundaries of the irradiated area in both directions. Such a defect might trap polishing compounds which would be extremely difficult if not impossible to remove by normal cleaning techniques. It is also possible that, with certain configurations, such features could exhibit damage by "self-focusing" at very high power.

Glass and fused silica surfaces are susceptible to impregnation by submicron size polishing compound particles during the polishing process. These particles may either get wedged into very small features on the surface (e.g., 10-20 Å), or may be partially embedded in the partially hydrolyzed gel-like skin of the polished $SiO_2$ surface. Some fusion or diffusion may also occur. It has been shown that such particles cannot be removed by jets of liquid or gas or by routine cleaning techniques; even further polishing may do nothing more than drive these particles toward the

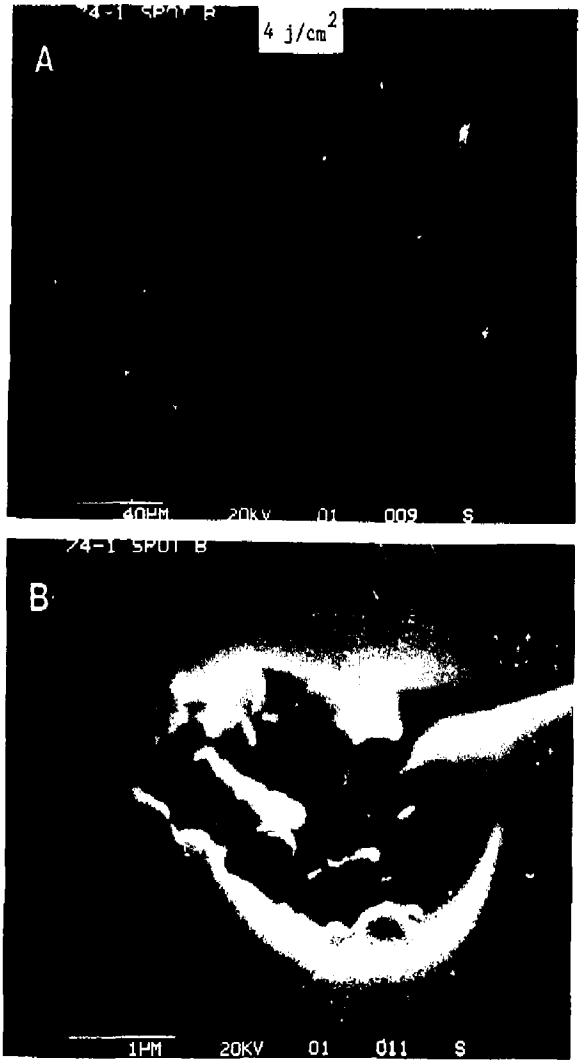


Figure 22 - Optical micrograph showing that laser damage sites are not associated with a crack originating from a particulate inclusion in the coating (A). Damage morphology of that particle as shown by scanning electron microscopy (B).

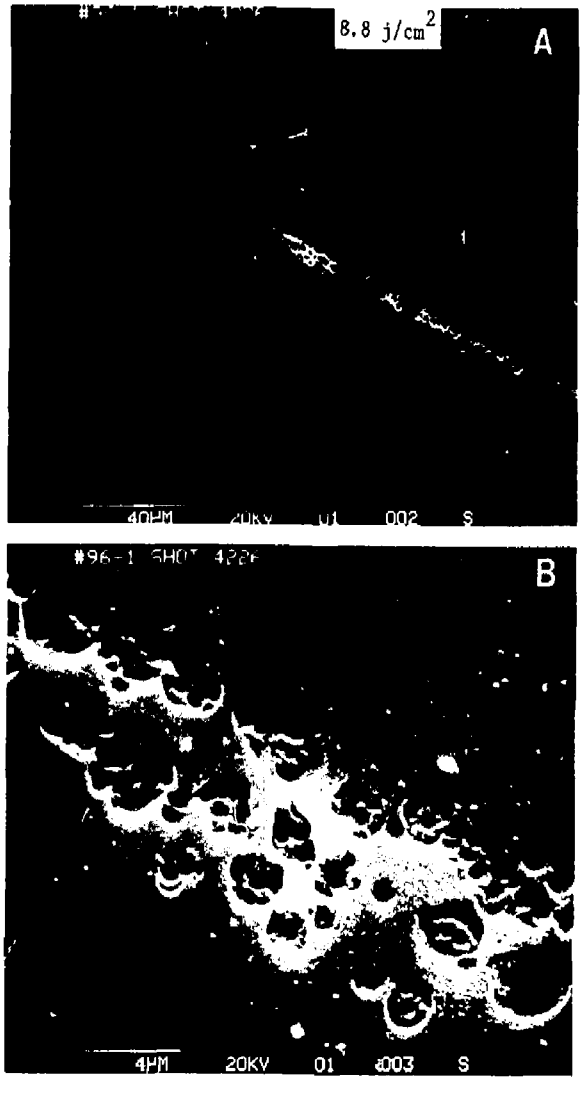


Figure 23 - Scanning electron micrograph of a linear array of damage sites in the $SiO_2$ coating coinciding with a polishing defect in the underlying substrate (A). Enlargement of these damage pits (B).

interior of the substrate. This type of absorbing site on the substrate surface may not show apparent damage unless it is covered by a coating. Only the blowout of the coating may make the interaction of the site with the laser visible. The effect of polishing on the damage threshold has been noted by Rainer, Milam, Lowdermilk and others.[40,41] They found that both fused silica and BK-7 glass showed significantly higher laser damage threshold values when the polishing was done by the "bowl-feed" method than by conventional polishing. The importance of polishing is confirmed in Table 5, where samples made using Zygo-polished substrates had damage thresholds of 3 to 9 $j/cm^2$, while the Unertl-polished substrates which were coated in the same batch damaged at 1.9 $j/cm^2$ or below.

Another important factor involved in laser damage is the formation of carbonaceous clusters in the coating during pyrolysis. The possibility of such an occurrence was clearly known, since the precursor solution contains alkly groups. However, efforts to analyze for carbon content of these films was frustrated by the thinness of coating and the low level of carbon. Finally, an exploratory investigation of the coating material obtained in bulk form through the gelling of the precursor coating solution revealed some very significant results.

The coating solution was found to show a tendency to form carbon upon pyrolysis. The carbon-forming tendency varied with such parameters as the way the components were mixed, firing rate, and firing schedule. (This is perhaps why there was wide scattering in our previous results). We looked into a number of ways of eliminating carbon formation, some of which included chemically dissolving the organic components before carbon formation, changes in the heating schedule, etc. We found several ways this could be done, but the simplest one, which does not require any additional steps in the process and equipment, was the extension of the hydrolysis/polymerization time from 16-24 hours to 60-72 hours at 60°C. This reduced the tendency to form carbon to the point of entirely eliminating it. Hydrolysis and polymerization reactions can also be accelerated by increasing the temperature and stirring or by refluxing the solution, provided that this is practical. Carbon

TABLE 5

EFFECT OF SUBSTRATE POLISHING AND OF MICRO SURFACTANT ON THE LASER DAMAGE THRESHOLD OF COATED SAMPLES

| Sample No. | Disc ID | Glass Type | Polish | Cleaning * | Drain Rate cm/min | Solution Age and Polymerization | Laser Damage Results ($j/cm^2$) |
|---|---|---|---|---|---|---|---|
| 23-1 | 85 | Corning 7940 | Westinghouse | Without MICRO | 5.0 | 4 days old 24 hrs at 60°C | DAMAGE: $3.1 \pm 0.5$ |
| 23-2 | 3626 | Suprasil | Westinghouse | Without MICRO | 5.0 | 4 days old 24 hrs at 60°C | DAMAGE: $2.8 \pm 0.3$ |
| 23-3 | 3629 | Suprasil | Zygo | Without MICRO | 5.0 | 4 days old 24 hrs at 60°C | DAMAGE: $3.3 \pm 0.5$ |
| 123-4 | 3621 | Suprasil | Zygo | Without MICRO | 5.0 | 4 days old 24 hrs at 60°C | DAMAGE: >9.06 |
| 123-5 | 3622 | Suprasil | Zygo | With MICRO | 4.0 | 2 days old 24 hrs at 60°C | DAMAGE: $3.3 \pm 0.3$ |
| 123-6 | 3630 | Suprasil | Zygo | With MICRO | 4.0 | 2 days old 24 hrs at 60°C | DAMAGE: $3.0 \pm 0.5$ |
| 123-7 | 86 | Corning 7940 | Unertl | With MICRO | 4.0 | 2 days old 24 hrs at 60°C | DAMAGE: $1.7 \pm 0.2$ |
| 123-8 | 79 | Corning 7940 | Unertl | With MICRO | 4.0 | 2 days old 24 hrs at 60°C | DAMAGE: $1.7 \pm 0.2$ |
| 123-9 | 36 | Corning 7940 | Unertl | Without MICRO | 4.0 | 2 days old 24 hrs at 60°C | DAMAGE: $1.9 \pm 0.4$ |
| 123-10 | 29 | Corning 7940 | Unertl | Without MICRO | 4.0 | 2 days old 24 hrs at 60°C | DAMAGE: $0.8 \pm 0.2$ |

*All samples were taken through the standard cleaning steps: (1) hot water ultrasonic; (2) rinse; (3) $H_2SO_4/H_2O_2$ soak; (4) rinse; (5) scrub; (6) rinse; (7) ethanol dry.
The table indicates that half of the samples used MICRO cleaning solution in steps (1) and (5), while the other half did not.

formation can be checked by pouring a small portion of the solution into a breaker, e.g., 1/4" deep, then gelling and drying it at room temperature. Upon firing, the materials which are subject to carbon formation turn black around 400°C. The materials which appeared to resist carbon formation under these conditions showed a weak tendency to form carbon by turning slightly yellow at the bottom of beaker when the beaker contained a larger amount of material. This indicates that it is very important that the material must see sufficient oxygen during the pyrolysis of organic components. For this reason, thicker coatings will have more of a tendency to form carbon below certain depths, and these carbonaceous residues will be located near the coating-substrate interface. Indeed, when coating thicknesses were reduced by reducing the solution drain rate from approximately 10 cm/min to 3-4 cm/min (∿450 nm vs ∿250 nm) the best damage thresholds suddenly doubled from 4-5 $j/cm^2$ to 9 $j/cm^2$.

However, it must be strongly emphasized that elimination of carbon formation in the coating does not guarantee high laser damage resistance. The multiplicity of the laser damage sources must be recognized. For example, when two samples which were coated using a drain rate of 4 cm/min ( ∿ 250 nm thick) were prepared as twins; that is, coated in succession with the same solution and heat-treated together, one of these samples showed a damage resistance of 9 $j/cm^2$ (118-2) while the other showed 1 $j/cm^2$(118-1). The only possible differences between these two samples can be in their substrates and in the substrate cleaning.

There is one other very important point. It was found that an organic-based component in our coating system, namely Tygon tubing, was contributing to carbon formation significantly. Solutions which did not form carbon as prepared did so after being run through the coating system containing this material.

The sources of laser damage in this process appear to fall into three major areas:

- Substrate preparation; i.e., polishing, cleaning, handling
- Coating solution chemistry and processing;i.e., carbon formation.
- Equipment and environment-induced effects; i.e., incompatible materials, inclusion of contaminants, etc.

All of these areas play a major role in contributing to laser damage, and their effects often overlap.

## APPENDIX A

### Tetraethylorthosilicate

The alkoxide used as a basis for the polymer solution is tetraethylorthosilicate (TEOS), $Si(OC_2H_5)_4$. We have been using reagent grade TEOS supplied by Fisher Scientific Co., Pittsburgh, PA, who began manufacturing their own material following their merger with Allied Chemicals a few years ago. A supplier which deals more routinely with large orders is Stauffer Chemicals Co. of Westport, CT, but we have no experience with their material. The table below does suggest, however, that their TEOS is similar to Fisher's.

Table 6

Comparison of TEOS from Two Manufacturers
(tests run by Stauffer)

| Test | Stauffer | Fisher |
|---|---|---|
| Monomer content | 99.8% | 99.9% |
| % HCl | <0.001 | <0.001 |
| APHA color test | 5 | 5 |
| Specific gravity (20°C) | 0.932 | 0.932 |
| Low boilers | trace | trace |
| High boilers | ~0.1 | 0.1 |

For this application, heavy metals content of the TEOS was a concern, and we analyzed the Fisher material using emission spectroscopy. The results showed that all of the elements considered, other than Si, were below the detection level. These included Al, Ag, B, Ba, Be, Bi, Ca, Co, Cr, Cu, Fe, Ga, Ge, K, Li, Mg, Mn, Mo, Na, Nb, Ni, Pb, Sb, Sn, Sr, Ti, V, Zn, and Zr.

The TEOS to be used in the coating solution for the large lenses has been ordered from Fisher. The order for 3500 gallons will

be shipped in epoxy-lined containers of 200 liters each. This order can be filled from a single factory batch, since each batch comprises 380 drums. Thus contamination by metals and reproducibility problems are avoided.

The ethyl silicate must be kept free of water at all times, since it hydrolyzes readily and self-polymerizes in a manner which conflicts with our purposes. It is planned that the 200-liter drums will be back-filled with dry nitrogen as liquid is pumped from them. However, two of the drums already received at LLNL have been tapped in order to test the purity of their contents. These were not back-filled with dry $N_2$, and the possibility of moisture contamination must not be ignored.

## Alcohol

The alcohol serves as a medium to disperse the reactive species. It must be 200 proof anhydrous ethyl alcohol and should be free of particulate matter. Since the water content of the coating solution is a critical parameter, the amount of water contained in the ethanol should be minimized. Anhydrous alcohol is usually "dried" by the manufacturer by additions of approximately 50 ppm benzene. Even so, water analysis by gas chromatography showed that freshly opened ethanol from two manufacturers had different water contents:

| ethanol supplier | volume % water |
|---|---|
| Pharmco | 0.18 |
| U.S. Industrial | 0.09 |

In addition, once humid air is allowed into the container, the alcohol continues to absorb moisture, even though the container is re-sealed:

| time after re-sealing (hrs) (Pharmco alcohol) | volume % water |
|---|---|
| 0 | 0.180 |
| 1.5 | 0.184 |
| 3.25 | 0.188 |

## 7. RECOMMENDATIONS

It was found that the carbon formation phenomenon in the precursor polymer solution is a complex one and that it has a direct bearing on the laser damage threshold of the resultant anti-reflective polymer oxide coating. Carbon formation appears to be influenced not only by the degree of hydrolysis and polymerization, mixing rates, and methods of reacting the ingredients, but also by post-formation factors such as aging, drying, and firing rates and atmospheres. It appears that there is a critical level of carbon which is detrimental at a given laser wavelength. There is also a critical thickness for the coating which facilitates burning of the carbonaceous materials to below the detrimental level. These observations lead to the following recommendation:

> A detailed scientific investigation directed toward the understanding of the above factors would not only be of immense scientific value in the field of oxide polymers but also is essential if these oxide polymers are to be used in high power lasers. Such a study is needed to ensure the reproducibility of the demonstrated 9 $j/cm^2$ damage threshold of the coatings at $3\omega$ and would be even more important if the laser system were to be operated at $4\omega$. Therefore, it is recommended that a major program be undertaken to investigate polymer solution chemistry, particularly the mechanism of carbon formation in organometallic-derived polymer oxides.

Thus one must keep a dry atmosphere over the alcohol as well as over the prepared coating solution in order to control water content.

It is instructive to note that the difference in total water content of the solution of 0.35 vol. % which results from using Pharmco versus USI alcohol makes no noticeable difference in the AR properties of the final coating. However, deliberate variations in the hydrolysis water of a solution prepared with 2.2 moles $H_2O$/mole TEOS compared to one with 2.0 moles caused significant changes in the pore structure and resulting AR properties of the final coating. This is equivalent to a change in water content of ~9.1 vol. %; keeping water fluctuations well below this level presents no problem.

## APPENDIX B

### Substrate Preparation

Efforts to pin down the minimum substrate preparation necessary to achieve acceptable laser damage resistance have been somewhat frustrated because of the large number of variables, but it has become clear that preparation of the substrate is a critical factor in producing a coated sample which will withstand a high-intensity UV laser.

Both Suprasil and Corning's 7940 glass appear to be acceptable substrates for damage-resistant coatings, provided that they are prepared properly prior to coating application. As discussed in section 6, care must be taken in polishing to see that defects are eliminated, but samples with damage thresholds above 5 $j/cm^2$ have been obtained using substrates which were ceria polished at Zygo Corporation and at Westinghouse R&D Optical Shop. Thresholds in the range of 2 to 3 $j/cm^2$ were typical of samples made with substrates polished at Unertl Optical Co. However, of the various methods employed to remove particulates from the glass surface before coating, only two have yielded damage-resistant coatings. One of these is scrubbing the surface with a soft nylon brush while flushing first with a surfactant in de-ionized water followed by plain de-ionized water. This process is presently done using an automatic scrubber of the type used in semiconductor manufacture, available from Solitec of Mountain View, CA. During the scrubbing step, both the substrate and the brush rotate at an estimated 500 rpm in opposite directions. This step is followed by a de-ionized water rinse, and drying is done by spinning. We have made a practice of coating the samples as soon as possible after scrubbing is done, usually within 30 minutes, in order to minimize the problem of dust from the atmosphere settling on the glass. This may not be necessary from the laser damage point of view, since samples which were cleaned at Westinghouse, sealed in nylon cases, hand carried to LLNL, and coated there, did show good laser damage resistance.

The second successful method of particulate removal is drag wiping, which has been in use at Lawrence Livermore National Labs for some time. This technique involves placing a lint-free Kodak lens tissue on the substrate, wetting it with a few drops of filtered, pure solvent such as ethanol or acetone, and dragging the tissue across the substrate surface.

Damage-resistant samples have been obtained using both spinning and draining as a means of depositing the coating, but only if the sample had been scrubbed or drag wiped before coating application. One puzzling problem is that attempts to reproduce these results by scrubbing at LLL with a Solitec brush, as described above, have been unsuccessful, yielding samples with low laser damage resistance. However, they have had good results with drag wiping.

Other methods of removing particles have been tested, but none has produced damage-resistant samples. Among these are high-power ultrasonic agitation at 20 kHz, overnight soak in $H_2SO_4$, and vapor deposition of propanol.

The observation that scrubbing or drag wiping before coating improves laser damage resistance, together with the "buckshot" distribution of damage sites (see Section 6), suggests that some absorbing particle is removed by the mechanical action. Such particles may be partially embedded in the $SiO_2$ surface, perhaps as part of a hydrated gelatinous layer believed to be generated during polishing, as suggested by N. Brown of Lawrence Livermore National Labs. If these particles are cerium oxide residue from polishing, chemical attack by dilute $H_2SO_4$ may be a practical removal method, provided that they are not protected from the acid by significant burial. This approach should be further investigated. It should be mentioned that the surfactant used during the scrubbing procedure is MICRO, a biodegradable, non-toxic product available from International Products Corporation, Trenton, NJ. A 2% solution of MICRO with de-ionized water has a pH of ~9.8, and the surfactant is reported to rinse clean in de-ionized water to a maximum of 33 parts per billion. However, recent suspicions regarding sodium residue which may not be removed by rinsing could lead to the elimination of MICRO in the cleaning procedure.

# WIDE SPECTRUM ANTIREFLECTIVE COATING FOR LASER FUSION SYSTEMS

B. E. Yoldas, D. P. Partlow, H. D. Smith*, D. M. Mattox
Westinghouse Research and Development Center
Pittsburgh, PA

*Westinghouse Hanford Company
Richland, WA

## ABSTRACT

A method of depositing a laser damage resistant, wide-spectrum antireflective coating on fused silica has been developed. This work was sponsored under a subcontract with the University of California, with technical direction from the Lawrence Livermore National Laboratory. The coating is applied from a specific silanol polymer solution and converted to a porous $SiO_2$ film. The pore size of the film is first reduced by a heat treatment to prevent UV scattering. Then gradation of the pore volume is achieved by a mild etching to a sufficient depth to provide a smoother index transition from air to the substrate glass. The resulting antireflectivity covers the entire transmission range of silica and may be extended to a wavelength as short as 250 nm. Laser damage thresholds as high as 9 $j/cm^2$ have been demonstrated on processed samples.

The coating is applied by immersing the substrate in the polymer solution and then either withdrawing the substrate or draining the solution at a predetermined rate to produce the desired film thickness. A computer-controlled system for the application of this coating on 80 cm NOVA laser lenses has been designed and built at the Westinghouse R&D Center and delivered to Lawrence Livermore Laboratory. The system can perform a series of processes, including solution preparation, coating application, heat treatment, and porosity grading.

In this report the formation of the wide spectrum antireflective coating on fused silica and the laser damage resistance of this coating at 350 nm are presented.

The scrubbing procedure presently used to clean polished substrates is as follows:

1. Ultrasonic agitation in a solution of 2% MICRO in water, kept ∿95°C for 5 min. This removes loose particles and polishing residue from the ground edges of the glass.

2. De-ionized water rinse.

3. Soaking in a mixture of 4 parts $H_2SO_4$ (full strength) to one part $H_2O_2$ (30%) for 1/2 hr. This step removes organic residue such as grease, oils, and hydrocarbon contamination from the atmosphere.

4. De-ionized water rinse.

5. Scrubbing with Solitec equipment as described above. This includes rinsing and spin-drying.

The drag-wiping procedure as described above is used alone, without any pre-cleaning or de-greasing.

The scaled-up equipment to be used for coating the 90 cm lenses at LLNL assumes that the lens is already free of organics and particulates. Thus no provision has been made thus far for scrubbing or for the $H_2SO_4/H_2O_2$ soak. Also, drying of the lens after a final water rinse is done by vapor deposition of a fluorinated hydrocarbon, Genesolv, which subsequently evaporates, leaving a water-free surface. The Genesolv process is also capable of removing particulates, since the droplets of dense liquid displace particles, which are carried away with the runoff. However, this cleaning step probably does not remove very small particles, which are held at the surface by considerable force, nor can it free embedded material.

## APPENDIX C

### Filtration

Filtration of the coating solution and/or its components is a practical means of removing unwanted particles which might lower the laser damage resistance of the fired film. Particles are also undesirable because they tend to be deposited on the substrate during the coating application process, causing irregularities in film thickness.

Experiments with various filtering materials have shown that cellulose and polycarbonate membranes swell upon contact with one or more of the solution components. The only membrane material which has been found to be compatible with all components as well as the prepared solution is PTFE (Teflon), which is available with pores as small as 0.02 μm. However, the prepared solution will not penetrate such small pores, and it flows exceedingly slowly through 0.10 μm pores, even under considerable pressure, suggesting that 0.10 μm filtration may be detrimental to the polymer unit integrity. Solutions were prepared from components which had been filtered at 0.02 μm, but the laser damage resistance of the subsequent fired films was similar to that obtained when 0.20 μm membranes were used. Since acceptable laser damage resistance has been attained by filtering only the prepared solution through a 0.20 μm PTFE membrane, and since interferometry done at LLL confirms the visual observation that these films are uniform in thickness, we have adopted this filtration scheme for our laboratory-scale operation. Cover gases which are used to protect the solution from moisture in the air are filtered in the same manner. The scaled-up equipment designed to coat the 90 cm optics uses disposable cartridge-type filters with a 0.20 μm PTFE membrane. As a precaution, all solution components are filtered, in addition to the cover gases and prepared solution. Figure 24 gives typical flow rates for methanol through this type of filter.

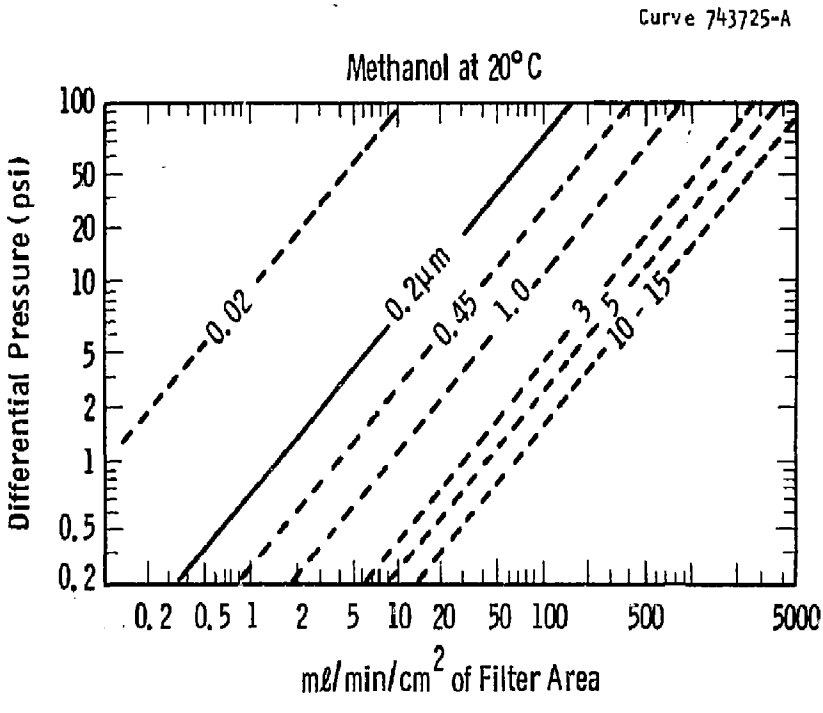


Figure 24 - Typical flow rates of methanol through PTFE filter membranes of various pore sizes at various pressures.

## REFERENCES


1. Lord Rayleigh, Proc. Roy. Soc. 41, 275 (1886).
2. J. Fraunhofer, in Glassmelting Handbook (Gesammelte Schriften), 35, E. Lommel, editor, Munich (1888).
3. H. D. Taylor, in The Adjustment and Testing of Telescope Objectives, 109, T. Book, editor, York, England (1894).
4. F. Kollmorgen, Trans. Illum. Eng. Soc. 11, 22 (1916).
5. M. P. Amy, Rev. Opt. 6, 305 (1927).
6. F. L. Jones and H. J. Homer, J. Opt. Soc. Am. 31, 34 (1941).
7. H. Schroder, Glastech. Ber. 20 (6), 161 (1942).
8. G. Bauer, Ann. Phys. 19, 434 (1934).
9. C. H. Cartwright, Phys. Rev. 57, 1060 (1940).
10. A. Smakula, Glastech. Ber. 19 (12), 377 (1941).
11. K. B. Blodgett, Phys. Rev. 55, 391 (1939).
12. F. H. Nicoll and F. E. Williams, U.S. Pat. 2,486,431, Nov. 1, 1949.
13. S. McLean, U.S. Pat. 2,639,999, May 26, 1953.
14. B. E. Yoldas, Appl. Opt., 19 (9), (1980).
15. S. P. Mukherjee and W. H. Lowdermilk, J. Non-Cryst. Solids 48, 177 (1982).
16. A. Smahuls, Glastech. Ber. 19 (12), 377 (1941).
17. K. B. Blodgett, Phys. Rev. 55, 391 (1939).
18. M. J. Minot, J. Opt. Soc. Am. 66, 515 (1976).
19. W. H. Lowdermilk and D. Milam, Appl. Phys. Lett. 36 (11), 891 (1980).

20. H. Schroeder, in Physics of Thin Films 5, 87, G. Hass and R. Thun, editors, Academic Press, New York (1969).

21. B. E. Yoldas and T. W. O'Keefe, Appl. Opt. 18, 3133 (1979).

22. B. E. Yoldas, Ibid 21 (16), 296 (1982).

23. Idem, J. Non-Cryst. Solids 51, 105 (1982).

24. Idem, J. Am. Ceram. Soc. 65, 388 (1982).

25. Idem, J. Mater. Sci. 14, 1843 (1979).

26. T. H. Elmer and F. W. Martin, Am. Ceram. Soc. Bull. 58 (11), 1092 (1979).

27. H. Shhroter, Ann. Physik. 39, 55 (1941).

28. R. Jacopsson, in Progress in Optics V, 249, E. Wolf, editor, North-Holland, Amsterdam (1966).

29. M. Born and E. Wolf, Principles of Optics, 55, Pergamon Press, New York (1975).

30. S. F. Monaco, J. Opt. Soc. Am. 51 (3), 280 (1961).

31. L. M. Cook and K.-H. Mader, Laser Focus, 73, March, 1983.

32. M. Bass, SPIE 76, 15 (1976).

33. N. Bloembergen, Appl. Opt. 12, 661 (1973).

34. M. J. Soileau, J. P. Porteus, P. A. Temple, and M. Bass, presented at the Fifth Laser Window Conference, Las Vegas, Nevada, Dec, 1975.

35. D. W. Fradin, "Laser Induced Damage in Solids," Ph.D. Thesis, Harvard University, March, 1973.

36. R. W. Hopper and D. R. Uhlmann, J. Appl. Phys. 41, 4023 (1970).

37. J. J. O'Dwyer, The Theory of Dielectric Breakdown in Solids, Oxford University Press, London (1964).

38. N. Bloembergen, Nonlinear Optics, W. A. Benjamin, Inc., New York (1965).

39. L. V. Keldysh, Sov. Phys. JETP 20, 1207 (1965).

40. D. Milam, W. H. Lowdermilk, F. Rainer, J. E. Swain, C. K. Carniglia, and T. Tuttle Hart, Appl. Opt. 21 (20), 3689 (1982).

41. F. Rainer, W. H. Lowdermilk, D. Milam, T. Tuttle Hart, T. L. Lichtenstein, and C. K. Carniglia, Ibid, 3685 (1982).